

OPTIMIZATION OF FRET METHOD TO DETECT DIMERIZATION OF  
DOPAMINE D2 AND ADENOSINE A2A RECEPTORS IN LIVE CELLS

A THESIS SUBMITTED TO  
THE GRADUATE SCHOOL OF NATURAL AND APPLIED SCIENCES  
OF  
MIDDLE EAST TECHNICAL UNIVERSITY

BY

GÖKHAN ÜNLÜ

IN PARTIAL FULFILLMENT OF THE REQUIREMENTS  
FOR  
THE DEGREE OF MASTER OF SCIENCE  
IN  
BIOLOGY

JULY 2011

Approval of the Thesis

**OPTIMIZATION OF FRET METHOD TO DETECT DIMERIZATION  
OF DOPAMINE D2 AND ADENOSINE A2A RECEPTORS IN LIVE  
CELLS**

Submitted by **GÖKHAN ÜNLÜ** in partial fulfillment of the requirement for the degree of **Master of Science in Biology Department, Middle East Technical University** by,

Prof. Dr. Canan Özgen  
Dean, Graduate School of **Natural and Applied Sciences** \_\_\_\_\_

Prof. Dr. Musa Doğan  
Head of the Department, **Biology** \_\_\_\_\_

Assist. Prof. Dr. Çağdaş D. Son  
Supervisor, **Biology Dept., METU** \_\_\_\_\_

**Examining Committee Members**

Prof. Dr. Meral Yücel  
Dept. of Biological Sciences, METU \_\_\_\_\_

Assist. Prof. Dr. Çağdaş D. Son  
Dept. of Biological Sciences, METU \_\_\_\_\_

Assist. Prof. Dr. A. Elif Erson Bengan  
Dept. of Biological Sciences, METU \_\_\_\_\_

Assist. Prof. Dr. Sreeparna Banerjee  
Dept. of Biological Sciences, METU \_\_\_\_\_

Assist. Prof. Dr. Hakan Kayır  
Dept. of Medical Pharmacology, GATA \_\_\_\_\_

**Date:** 05/07/2011

**I hereby declare that all information in this document has been obtained and presented in accordance with academic rules and ethical conduct. I also declare that, as required by these rules and conduct, I have fully cited and referenced all material and results that are not original to this work.**

Name, Last name : Gökhan ÜNLÜ

Signature :

## ABSTRACT

### OPTIMIZATION OF FRET METHOD TO DETECT DIMERIZATION OF DOPAMINE D<sub>2</sub> AND ADENOSINE A<sub>2A</sub> RECEPTORS IN LIVE CELLS

Ünlü, Gökhan

M.Sc., Department of Biology

Supervisor: Assist. Prof. Dr. Çağdaş D. Son

July 2011, 89 pages

Recent studies demonstrate that there are several G-protein coupled receptors (GPCRs) that dimerize with other GPCRs and form heterodimers. Adenosine A<sub>2A</sub>-Dopamine D<sub>2</sub> receptor interaction is one of the examples for GPCR heterodimerization. Both receptors bear critical roles in physiological processes. Adenosine A<sub>2A</sub> receptor has functions in neurotransmission, cardiovascular system and immune response. On the other hand, dopamine receptors are the key point of dopaminergic system, which controls the regulation of memory, attention, food intake, endocrine regulation, psychomotor activity and positive reinforcement. Deregulation in dopamine signaling could cause neurological disorders such as Parkinson's disease and schizophrenia. Dopamine D<sub>2</sub>R and adenosine A<sub>2A</sub>R have been shown to interact in striatum and modulate dopaminergic activity.

The purpose of this study is to optimize Fluorescence Resonance Energy Transfer (FRET) method to detect dimerization of D<sub>2</sub>R and A<sub>2A</sub>R by tagging them with EGFP (enhanced green fluorescent protein) and mCherry (a red fluorescent protein) in live N2a cell line using laser scanning confocal microscope. Establishing this model will pave the ways for understanding mechanisms of interaction between dopamine and adenosine signaling, thereby, contributing to the understanding molecular mechanisms of some neurophysiological events and disorders. Moreover, the fluorescence based live cell model will be used to detect effects of potential anti-psychotic drugs on the interaction of these two receptors.

Indeed, follow-up studies are necessary to extend the limits of this project. Further imaging analyses and drug-receptor interaction studies can be readily applied to extract more information on dopamine-adenosine signaling by using the system developed with this thesis study.

Keywords: Dopamine D<sub>2</sub>R, Adenosine A<sub>2A</sub>R, GPCR Heterodimerization, FRET

## ÖZ

### CANLI HÜCRELERDE DOPAMİN D<sub>2</sub> VE ADENOZİN A<sub>2A</sub> RESEPTÖRLERİNİN EŞLEŞMELERİNİN FRET METODU İLE TESPİTİNİN OPTİMİZASYONU

Ünlü, Gökhan

Yüksek Lisans, Biyoloji Bölümü

Tez Yöneticisi: Yrd. Doç. Dr. Çağdaş D. Son

Temmuz 2011, 89 sayfa

Güncel çalışmalar, birçok G-proteine kenetli reseptörün (GPKR) diğer GPKR'ler ile eşleşip heterodimerler oluşturduğunu ileri sürmektedir. Adenozin A<sub>2A</sub> ve dopamine D<sub>2</sub> reseptör etkileşimi GPKR heterodimerizasyonuna bir örnek teşkil etmektedir. Her iki reseptör de fizyolojik olaylarda kritik roller oynamaktadır. Adenozin A<sub>2A</sub> reseptörünün, sinirsel iletim, kardiyovasküler sistem ve vücudun bağışıklık sisteminde görevleri vardır. Öte yandan dopamin reseptörleri, hafızanın düzenlenmesini, dikkati, besin alımını, endokrin düzenlenmesini, psikomotor aktiviteleri ve pozitif takviyeyi kontrol eden dopaminerjik sistemin anahtar noktasıdır. Dopamin sinyal yolağındaki düzensizlikler Parkinson hastalığı ve şizofreni gibi nörolojik bozukluklara yol açabilir. Dopamine D<sub>2</sub> ve adenozin A<sub>2A</sub> reseptörlerinin striatumda eşleştikleri ve dopaminerjik aktiviteyi düzenledikleri gösterilmiştir.

Bu çalışmanın amacı; D<sub>2</sub>R ve A<sub>2A</sub>R eşleşmesini tespit etmek için canlı N2a hücrelerinde bu reseptörleri EGFP (geliştirilmiş yeşil floresan protein) ve mCherry (kırmızı floresan protein) floresan proteinleriyle işretmek ve lazer taramalı konfokal mikroskop kullanarak Floresan Rezonans Enerji Transferi (FRET) yöntemini optimize etmektir. Bu model, dopamin-adenozin sinyal yollarının etkileşimlerinin mekanizmalarını anlamak için yeni yollar açacaktır. Böylelikle, bazı nörofizyolojik olayların ve bozuklukların da moleküler mekanizmalarının anlaşılmasına katkıda bulunulacaktır. Ayrıca tasarlanan floresan tabanlı canlı hücre modeli, potansiyel anti-psikotik ilaçların bu iki reseptörün eşleşmesi üzerine etkilerinin tespiti için kullanılabilir.

Elbette ki bu projenin sınırlarının genişletilmesi için çalışmalarının devam etmesi gerekmektedir. İleride yapılacak görüntüleme, analiz ve ilaç-reseptör etkileşimi çalışmaları geliştirilen bu sistem kullanılarak kolayca uygulanabilir ve bu model sayesinde dopamin-adenozin sinyal iletimleriyle ilgili daha fazla bilgiye ulaşılabilir.

Anahtar Kelimeler: Dopamin D<sub>2</sub>R, Adenozin A<sub>2A</sub>R, GPKR Heterodimerizasyonu, FRET

To my family

## ACKNOWLEDGEMENTS

I would firstly like to present my deepest gratitude to my supervisor Assist. Prof. Dr. Çağdaş D. SON, without whom this thesis study would be neither started nor completed. I owe him a lot for his endless moral support, guidance, encouragement, tolerance, patience and understanding. I cannot feel luckier to work with such a great mentor. I will always be grateful to him in my entire academic life.

I also want to thank the members of thesis examining committee; Prof. Dr. Meral Yücel, Assist. Prof. Dr. A. Elif Erson Bensan, Assist. Prof. Dr. Sreeparna Banerjee, Assist. Prof. Dr. Hakan Kayır for evaluating this thesis; and their invaluable suggestions and comments to make the final version of this thesis better.

I should also acknowledge the members of SON's Lab., all of whom supported, trusted and believed me to complete this Master's thesis. I appreciate their efforts to make SON's Lab. be a better place and working environment not only scientifically, but also socially.

I would like to thank METU Central Laboratory, Molecular Biology, Biotechnology R&D Center and UNAM for Confocal Microscopy Facilities which allowed taking confocal microscopy images presented in this study.

I should here mention the contributions of Assist. Prof. Dr. A. Elif ERSON BENSAN and Prof. Dr. Henry LESTER who kindly gifted pcDNA 3.1 (-) vector; Enhanced Green Fluorescent Protein (EGFP) and mCherry cDNA

vectors, respectively. I would also like to thank Assist. Prof. Dr. Tlin YANIK for providing N2a cell line used in this project.

I cannot complete this thesis without thanking my dearest friends; Ahu İzgi, Alper Mutlu, Çaęrı Urfalı, Damla Gldaę, Ezgi Eroęlu, İbrahim Sertdemir and Yaęmur Mięooęulları, without whom I could not progress this far to the end of this thesis study. They are not only friends but also advisors to me. They always supported, helped and cheered me up in hard times. They also aided a lot in scientific discussions about my project and gave advises to make some procedures better and easier. I can say by heart that these two years of master study would not be so good without their friendship. I deeply thank them for always being there for me and helping me at all times.

Last but not the least; I would like to express my thanks to my parents, Nuran and Fikret NL and my sisters Eda ERSZ and Funda MERCİMEK for believing and encouraging me throughout all my education years and being my first teachers and advisors. They are who prepared me for science and taught very basics of my knowledge in the first place.

Finally, I acknowledge TBİTAK for financially supporting me with TBİTAK BİDEB 2210 –Domestic Master Scholarship Program.

This work is supported by Marie Curie Actions, International Reintegration Grant (IRG) and METU internal research funds with the project number BAP-08-11-2010-R17.

## TABLE OF CONTENTS

ABSTRACT.....	iv
ÖZ.....	vi
ACKNOWLEDGEMENTS.....	ix
TABLE OF CONTENTS.....	xi
LIST OF TABLES.....	xiv
LIST OF FIGURES.....	xv
LIST OF ABBREVIATIONS.....	xviii
CHAPTERS	
1. INTRODUCTION.....	1
1.1. G-Protein Coupled Receptors.....	1
1.1.1. Dopamine Signaling.....	3
1.1.1.1. Dopamine D <sub>2</sub> Receptor.....	5
1.1.2. Adenosine Signaling.....	6
1.1.2.1. Adenosine A <sub>2A</sub> Receptor.....	10
1.2. Interaction of Adenosine A <sub>2A</sub> and Dopamine D <sub>2</sub> Receptors.....	10
1.3. Dimerization of G-Protein Coupled Receptors.....	11
1.3.1. Methods to Detect Dimerization of G-Protein Coupled Receptors.....	14
1.3.1.1. Fluorescence (Förster) Resonance Energy Transfer.....	15
1.4. Aim of the Study.....	18
2. MATERIALS & METHODS.....	20
2.1. Materials.....	20
2.1.1. Neuro2a (N2a) Mouse Neuroblastoma Cell line and Media.....	20
2.1.2. Neuro2a Cell Culture Conditions.....	21
2.1.3. Bacterial Culture Media and Conditions.....	21

2.1.4. Other Chemicals and Materials.....	22
2.2. Methods .....	23
2.2.1. Preparation of Competent <i>E. coli</i> Cells by CaCl <sub>2</sub> Method .....	23
2.2.2. Transformation of Competent <i>E. coli</i> Cells with a Plasmid .....	23
2.2.3. Restriction Enzyme Digestion .....	24
2.2.4. Ligation.....	25
2.2.5. Polymerase Chain Reaction (PCR).....	25
2.2.6. Agarose Gel Electrophoresis .....	26
2.2.7. Extraction of DNA from Agarose Gel.....	26
2.2.8. Quantification of DNA Amount .....	26
2.2.9. PCR Integration Method.....	26
2.2.10. Transfection of N2a Cells with pcDNA 3.1 (-) Eukaryotic Expression Vector .....	28
2.2.11. Imaging Transfected N2a Cells with Laser Scanning Confocal Microscope.....	29
2.2.12. Image Analysis with Pix-FRET .....	30
3. RESULTS & DISCUSSION .....	31
3.1. Cloning of <i>DRD2</i> coding sequence from pDONR221 to pDNR-Dual vector .....	32
3.2. Tagging A <sub>2A</sub> Receptor with mCherry Using PCR Integration Method.....	34
3.3. Cloning of A <sub>2A</sub> R and D <sub>2</sub> R cDNAs to pcDNA 3.1 (-) Mammalian Expression Vector.....	44
3.4. Tagging Dopamine D <sub>2</sub> Receptor with mCherry and EGFP Using PCR Integration Method.....	47
3.5. Tagging A <sub>2A</sub> R and D <sub>2</sub> R with EGFP .....	52
3.6. Optimization of Fluorescence Resonance Energy Transfer in N2a Cells Double Transfected with A <sub>2A</sub> R-EGFP & D <sub>2</sub> R-mCherry .....	57
4. CONCLUSION.....	65
REFERENCES .....	67

## APPENDICES

A. METABOLIC REACTIONS.....	75
B. NEURO2A CELL CULTURE MEDIUM.....	79
C. BACTERIAL CELL CULTURE MEDIA PREPARATION.....	81
D. BUFFERS & SOLUTIONS.....	82
E. PLASMID MAPS.....	84
F. REPRESENTATIVE 3D STRUCTURES OF RECEPTORS FUSED WITH FLUORESCENT PROTEINS.....	87
E. PRIMERS.....	88

## LIST OF TABLES

### TABLES

<b>Table 1.1</b>	Summary of adenosine receptor subtypes.....	9
<b>Table 2.1</b>	Optimized PCR conditions to amplify fluorescent protein coding sequences .....	25
<b>Table 2.2</b>	Conditions for PCR integration method.....	27
<b>Table B.1</b>	Composition of D-MEM with High Glucose .....	79

## LIST OF FIGURES

### FIGURES

<b>Figure 1.1</b> GPCR signaling on a diverse range of ligands .....	2
<b>Figure 1.2</b> Structure of dopamine .....	3
<b>Figure 1.3</b> Structure of adenosine .....	6
<b>Figure 1.4</b> Spectroscopic characteristics of EGFP and mCherry .....	17
<b>Figure 2.1</b> Experimental strategies outlining the methods of designing fluorescently tagged receptors .....	28
<b>Figure 3.1</b> PCR product of <i>DRD2</i> cDNA with RE ends .....	32
<b>Figure 3.2</b> <i>SalI</i> and <i>HindIII</i> digestion products of D <sub>2</sub> R PCR product and pDNR-Dual_A <sub>2A</sub> Rvector .....	33
<b>Figure 3.3</b> PCR to amplify D <sub>2</sub> R gene from isolated plasmids of ligation of D <sub>2</sub> R to pDNR-Dual vector.....	34
<b>Figure 3.4</b> Agarose gel electrophoresis photo of mCherry PCR amplification with A <sub>2A</sub> flanking ends .....	35
<b>Figure 3.5</b> Agarose gel photo of PCR product of mCherry amplified from pDNR-Dual_A <sub>2A</sub> R .....	36
<b>Figure 3.6</b> Map of pDNR-Dual vector .....	37
<b>Figure 3.7</b> Map of pcDNA 3.1 (-) .....	38
<b>Figure 3.8</b> <i>NotI</i> and <i>HindIII</i> digested pDNR-Dual_A <sub>2A</sub> R + mCherry and pcDNA 3.1 (-) with a 2 kb insert.....	39
<b>Figure 3.9</b> Agarose gel photo of mCherry PCR to screen potential pcDNA 3.1 (-)_A <sub>2A</sub> R + mCherry plasmids.....	40
<b>Fig. 3.10</b> Agarose gel photo of <i>NotI</i> and <i>HindIII</i> double digested pcDNA 3.1 (-)_A <sub>2A</sub> R + mCherry .....	41
<b>Figure 3.11</b> Coding sequence of A <sub>2A</sub> R+mCherry fusion .....	42

<b>Figure 3.12</b> N2a cells transfected with pcDNA 3.1 (-)_A <sub>2A</sub> R+mCherry vector excited at 543 nm .....	43
<b>Figure 3.13</b> pcDNA 3.1 (-), pDNR-Dual_A <sub>2A</sub> R and pDNR-Dual_D <sub>2</sub> R that were cut with <i>NotI</i> and <i>HindIII</i> .....	44
<b>Figure 3.14</b> pcDNA 3.1 (-)_D <sub>2</sub> R plasmids (lane 1-2) digested with <i>NotI</i> and <i>HindIII</i> .....	45
<b>Figure 3.15</b> Agarose gel photo of PCR products of pcDNA 3.1 (-)_D <sub>2</sub> R plasmids .....	46
<b>Figure 3.16</b> Agarose gel photo of <i>NotI-HindIII</i> digestion products of pcDNA 3.1 (-)_A <sub>2A</sub> R plasmids .....	47
<b>Figure 3.17</b> Agarose gel electrophoresis photo of EGFP and mCherry PCR amplification with D <sub>2</sub> R flanking ends .....	48
<b>Figure 3.18</b> Agarose gel photo of <i>NotI-HindIII</i> digestion screening of candidate pcDNA 3.1 (-)_D <sub>2</sub> R-EGFP/mCherry vectors .....	49
<b>Figure 3.19</b> N2a cells transfected with pcDNA 3.1 (-)_D <sub>2</sub> R+mCherry vector, excited at 543 nm .....	50
<b>Figure 3.20</b> Coding sequence of D <sub>2</sub> R+mCherry fusion gene.....	51
<b>Figure 3.21</b> Agarose gel electrophoresis photo of EGFP PCR amplification with A <sub>2A</sub> and D <sub>2</sub> R flanking ends.....	52
<b>Figure 3.22</b> Agarose gel photo of <i>NotI-HindIII</i> digestion screening of candidate pcDNA 3.1 (-)_D <sub>2</sub> R-EGFP & pcDNA 3.1 (-)_A <sub>2A</sub> R-EGFP vectors .....	53
<b>Figure 3.23</b> N2a cells transfected with pcDNA 3.1 (-)_A <sub>2A</sub> R+EGFP#1 and pcDNA 3.1 (-)_D <sub>2</sub> R+EGFP#1' vectors, excited at 458 nm .....	54
<b>Figure 3.24</b> Coding sequence of A <sub>2A</sub> R+EGFP fusion gene .....	55
<b>Figure 3.25</b> Coding sequence of D <sub>2</sub> R+EGFP fusion gene .....	56
<b>Figure 3.26</b> Track 1 configuration in laser scanning confocal microscope .....	58
<b>Figure 3.27</b> Track 2 configuration in laser scanning confocal microscope .....	59
<b>Figure 3.28</b> Track 3 configuration in laser scanning confocal microscope .....	60
<b>Figure 3.29</b> N2a cells transfected with A <sub>2A</sub> R-mCherry .....	62

<b>Figure 3.30</b> N2a cells transfected with D <sub>2</sub> R-EGFP.....	62
<b>Figure 3.31</b> N2a cells transfected with D <sub>2</sub> R-EGFP and A2AR-mCherry.....	63
<b>Figure A.1</b> Metabolic reactions of dopamine.....	75
<b>Figure A.2</b> Intracellular metabolism of adenosine.....	76
<b>Figure A.3</b> Extracellular metabolism of adenosine.....	77
<b>Figure A.4</b> Conversion of ATP to cAMP by the action of adenylyl cyclase...	78
<b>Figure E.1</b> Map of pDNR Dual vector.....	84
<b>Figure E.2</b> Map of pcDNA 3.1 (-) .....	85
<b>Figure E.2</b> Map of pDONR221.....	86
<b>Figure F.1</b> Representative 3D structures of receptor fusions.....	87

## LIST OF ABBREVIATIONS

A <sub>2A</sub> R	Adenosine A <sub>2A</sub> Receptor
AC	Adenylyl Cyclase
ADHD	Attention Deficit Hyperactive Disorder
ADP	Adenosine Diphosphate
AMP	Adenosine Monophosphate
ATP	Adenosine Triphosphate
bp	base pair
BiFC	Bimolecular Fluorescence Complementation
BRET	Bioluminescence Resonance Energy Transfer
BSA	Bovine Serum Albumin
cAMP	cyclic AMP
CFP	Cyan Fluorescent Protein
CCR5	C-C Chemokine Type 5 Receptor
cDNA	Complementary Deoxyribonucleic Acid
CNS	Central Nervous System
CoIP	Co-Immunoprecipitation
D-MEM	Dulbecco's Modified Eagle Medium
D-PBS	Dulbecco's Phosphate Buffered Saline
DNA	Deoxyribonucleic Acid
EDTA	Ethylenediamine tetraacetic acid
EGFP	Enhanced Green Fluorescent Protein
ER	Endoplasmic Reticulum
FRET	Fluorescence/Förster Resonance Energy Transfer
G <sub>i</sub>	Inhibitory G <sub>α</sub> subunit
G <sub>olf</sub>	Olfactory G <sub>α</sub> subunit

G <sub>s</sub>	Stimulatory G <sub>α</sub> subunit
GABA	γ-amino Butyric Acid
GDP	Guanosine Diphosphate
GFP	Green Fluorescent Protein
GIRK	G-protein gated inward rectifying potassium channels
GnRH	Gonadotropin Releasing Hormone
GPCR	G-Protein Coupled Receptor
GTP	Guanosine Triphosphate
<i>Hin</i>	<i>Haemophilus influenzae</i>
IL	Interleukin
kb	Kilobase pair
LB	Luria Bertani
MAP	Mitogen Activated Protein
mCherry	monomericCherry
mGluR	Metabotropic Glutamate Receptor
mRNA	Messenger Ribonucleic Acid
N2a	Neuro2a
<i>Not</i>	<i>Nocardia otitidis-caviarum</i>
PBS	Phosphate Buffered Saline
PCR	Polymerase Chain Reaction
PLC	Phospholipase C
PLD	Phospholipase D
RE	Restriction Enzyme
rpm	Revolution per Minute
<i>Sal</i>	<i>Streptomyces albus</i>
<i>Taq</i>	<i>Thermus aquaticus</i>
TBE	Tris Borate EDTA
UV	Ultraviolet
YFP	Yellow Fluorescent Protein

## CHAPTER I

### INTRODUCTION

#### 1.1 G-Protein Coupled Receptors

G-protein coupled receptor superfamily comprises the largest cell surface protein family (Kobilka, 2007). There are approximately 1000 genes encoding G-protein coupled receptors (GPCRs) in the human genome (Takeda, Kadowaki, Haga, Takaesu, & Mitaku, 2002). GPCRs share the common structure of 7 transmembrane segments, extracellular N-terminus and intracellular C-terminus (Kobilka, 2007). This receptor superfamily can be classified into 5 main families depending on the similarities of their seven-transmembrane segment sequences. The rhodopsin, adhesion, frizzled/taste2, glutamate and secretin families all together constitute the G-protein coupled receptor superfamily (Fredriksson, Lagerström, Lundin, & Schiöth, 2003). Having such members, GPCRs play important roles in cellular processes such as neurotransmission, cellular differentiation, inflammation, immune response and cell growth. GPCRs accomplish these functions by binding to a diverse range of ligands as neurotransmitter, light, odorants, biological amines, chemokines, peptides, amino acids and nucleosides (Bouvier, 2001). Upon ligand binding, GPCRs are activated and transduce the signal to a heterotrimeric G-protein, composed of three subunits,  $\alpha$ ,  $\beta$  and  $\gamma$ . Ligand binding to a GPCR activates the bound heterotrimeric G-protein by catalyzing the exchange reaction of GDP with GTP; thereby leading a conformational change in  $G_{\alpha}$ , but not in  $G_{\beta\gamma}$  subunit

(Lambright et al., 1996). Through dissociation of  $G_\alpha$  and  $G_{\beta\gamma}$ , a G-protein can activate or inhibit several distinct effectors such as enzymes, ion channels (Neer, 1995); and other intracellular signal cascades like MAP kinase pathway (Crespo, Xu, Simonds, & Gutkind, 1994). Stimulation or inhibition of these effector molecules like adenylyl cyclase, phospholipase C and ion channels results in changes in the levels of such secondary messengers as cAMP and calcium (Strader, Fong, Tota, Underwood, & Dixon, 1994).

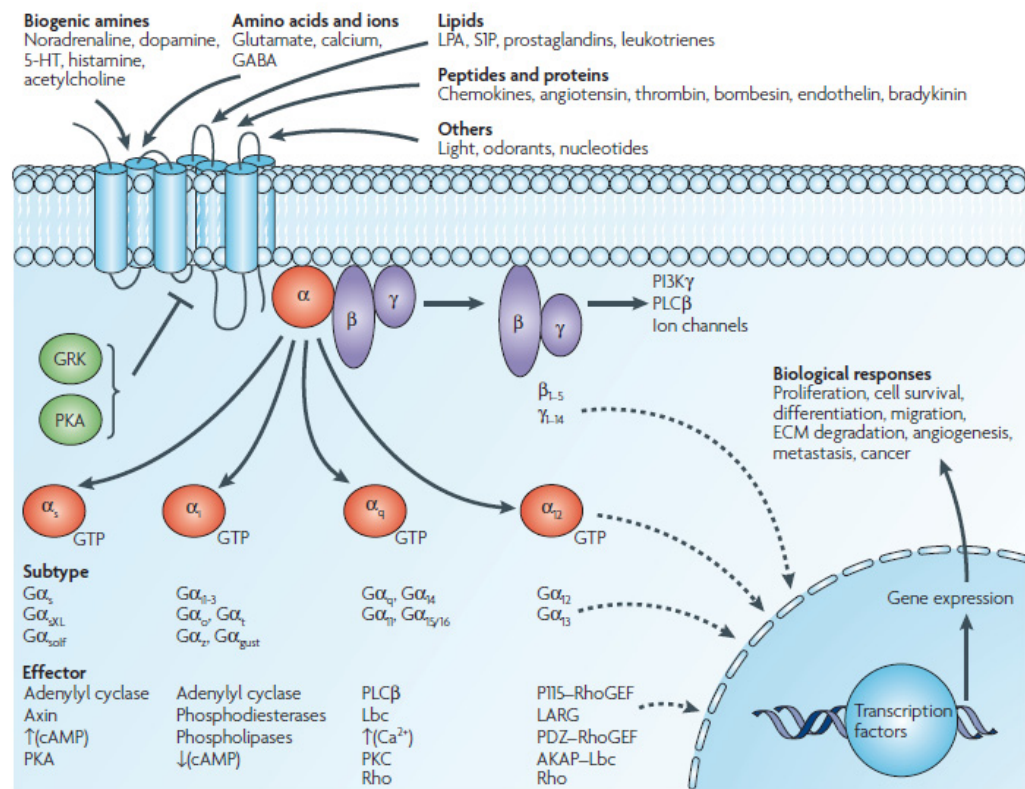


**Figure 1.1** GPCR signaling on a diverse range of ligands and the downstream signaling of distinct GPCR pathways (taken from (Dorsam & Gutkind, 2007))

More than 50% of drugs in market are targeted at G-protein coupled receptors and sales of these drugs exceeded 30 billion dollars in 2001 (Klabunde & Hessler, 2002). To exemplify, agonists and antagonists of different GPCRs are currently used against asthma, heart failure, hypertension, allergies, migraine and psychotic disorders (Bouvier, 2001).

### 1.1.1 Dopamine Signaling

Dopamine, a catecholamine derivative neurotransmitter, acts through dopamine receptors which are the members of G-protein coupled receptor superfamily. To date, five dopamine receptors have been characterized and have been divided into two subfamilies; D1- like and D2-like dopamine receptors. The D1-like receptors are of two types, D1 and D5 dopamine receptors; whereas, D2-like subfamily contains three receptors, namely, D2, D3 and D4 dopamine receptors (Gingrich & Caron, 1993).

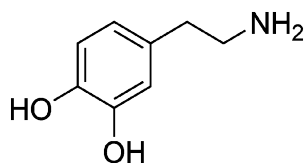


**Figure 1.2** Structure of dopamine (see Appendix A for metabolic reactions)

Dopamine receptors can show their effects on intracellular effectors via heterotrimeric GTP-binding proteins (Hepler & Gilman, 1992). Especially, third

intracellular loops of dopamine receptors are involved in receptor-G-protein interaction (Strader, Sigal, & Dixon, 1989). Activated G-proteins, in turn, either stimulate or inhibit the cAMP pathway or modulate calcium signaling. Subfamilies of dopamine receptors are different from each other in terms of their effects on cAMP pathway. D1-like receptors positively regulate adenylyl cyclase (AC) to produce more cAMP (Jackson & Westlind-Danielsson, 1994). Increased cAMP levels result in the activation of protein kinase A (PKA), which, in turn, phosphorylates many proteins in the cell to regulate cellular metabolism. The series of events occurring under the control of PKA also causes neurotransmitter release (Choi, Xia, Villacres, & Storm, 1993). On the other hand, D2-like dopamine receptors negatively regulate AC, and thus, decrease cAMP levels (Jackson & Westlind-Danielsson, 1994). Another difference between D1- and D2-like receptors comes from structural aspects. Third intracellular loops of D2-like receptors are considerably long, which is a specificity of the receptors that interact with inhibitory  $G_{\alpha}$ , also known as  $G_i$ , to inhibit AC; whereas, D1-like receptors have short third intracellular loops like other GPCRs coupling to stimulatory  $G_{\alpha}$ , also known as,  $G_s$  (Civelli, Bunzow, & Grandy, 1993).

Neurotransmission through dopamine signaling bears very fundamental roles in various neural processes such as cognition, learning, emotion, reward and motor function (Rashid, O'Dowd, Verma, & George, 2007). Having such important functions, deregulation of dopamine receptor signaling leads to several metabolic disorders like Parkinson's disease, Tourette's syndrome, schizophrenia, attention deficit hyperactive disorder (ADHD) and pituitary tumor generation (Vallone, Picetti, & Borrelli, 2000). Antagonists of dopamine receptors have been designed to block hallucinations and delusions that are the symptoms of schizophrenia; on the other hand, agonists have diminishing effects of hypokinesia seen in patients with Parkinson's disease (Missale, Nash, Robinson, Jaber, & Caron, 1998).

### 1.1.1.1 Dopamine D<sub>2</sub> Receptor

Dopamine D<sub>2</sub> receptor has two alternatively spliced forms which differ from each other only by a 29 amino acid insertion in the third intracellular loop. These two forms are called short and long variants, D<sub>2S</sub> and D<sub>2L</sub> (Dal Toso et al., 1989). Even though, the amino acid insertion is located on such a critical interaction site as third intracellular loop, no functional diversity has been revealed between the two (Missale, et al., 1998). They are both coupled to G<sub>i/o1f</sub>; and therefore, have inhibitory effects on adenylyl cyclase when they are expressed in cell lines; however, D<sub>2S</sub> receptor showed a higher affinity than D<sub>2L</sub> (Dal Toso, et al., 1989).

Among many other functions shared by all dopamine receptor subtypes, D<sub>2</sub>R gene (*DRD2*) is associated with alcoholism (Thanos et al., 2005), co-morbid depression, anxiety and social dysfunction in untreated veterans with post-traumatic stress disorder (Lawford, Young, Noble, Kann, & Ritchie, 2006). The activity of this receptor does also modulate Akt signaling by suppressing it and its downstream effector, GSK-3 $\beta$  (Glycogen synthase kinase-3 $\beta$ ). This suppression alters development of GABAergic neurons in zebrafish larvae as a result of decreasing the size of GABAergic neurons (Souza, Romano-Silva, & Tropepe, 2011). Apart from Akt signaling, D<sub>2</sub>R activation can selectively inhibit Wnt pathway through direct interaction with  $\beta$ -catenin (Min et al., 2011). Activation of Wnt pathway controls the level of  $\beta$ -catenin present in the cytosol, which can go to the nucleus and serves as a transcriptional co-activator for transcription factor LEF/TCF (lymphoid enhancing factor/T-cell factor) (Cadigan & Liu, 2006).

D<sub>2</sub> receptors are also present in cardiac tissue and their activation with an agonist decreases heart rate and arterial blood pressure (Végh, Papp, Semeraro, Fatehi-Hasanabad, & Parratt, 1998). In another recent article, it has been shown

that D2 receptors activation can prevent cardiomyocytes from apoptosis caused by ischemia/reperfusion damage (Li et al., 2011).

### 1.1.2 Adenosine Signaling

Adenosine is a purinergic messenger that modulates many cellular processes in the organs of both central and peripheral nervous systems (Dunwiddie & Masino, 2001). As a chemical messenger molecule, adenosine acts through four receptor subtypes all of which belong to G-protein coupled receptor superfamily; namely, A<sub>1</sub>, A<sub>2A</sub>, A<sub>2B</sub>, A<sub>3</sub> receptors (Olah & Stiles, 1995).

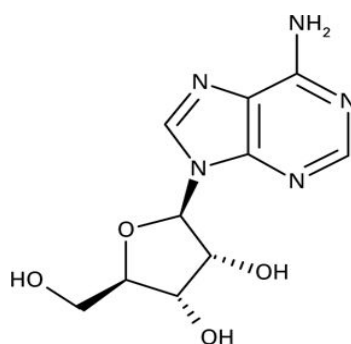


**Figure 1.3** Structure of adenosine (see Appendix A for metabolic reactions)

Upon activation of these receptors, adenosine signaling is involved in multiple metabolic functions such as modulation of excitability in the CNS, mechanisms of seizure susceptibility, induction of sleep, perception of pain, respiration and cerebral blood flow (Benarroch, 2008). Because of these important metabolic functions, adenosine receptors have become a very important drug target against

cerebral ischemia (Ribeiro, 2005), pain (Sawynok & Liu, 2003), seizures (During & Spencer, 1992), Parkinson disease (Schapira et al., 2006) and Huntington disease (Blum, Hourez, Galas, Popoli, & Schiffmann, 2003). Inhibitors used as drugs for adenosine receptors mostly include caffeine and methylxanthine derivatives (Benarroch, 2008).

Adenosine  $A_1$  and  $A_{2A}$  receptors are highly abundant in nervous system; and most physiological functions have mainly been fulfilled by these two receptors.  $A_1R$  is coupled to inhibitory  $G_\alpha$  subunit, also known as,  $G_i$  which inhibits adenylyl cyclase activity and decreases cAMP levels. It also activates potassium ( $K^+$ ) channels to increase  $K^+$  conductance; and inhibits presynaptic calcium ( $Ca^{2+}$ ) channels.  $A_1$  receptor activation has a global inhibitory regulation on synaptic transmission (Ribeiro, 2005). On the other hand,  $A_{2A}$  receptors are coupled to stimulatory type  $G_\alpha$ , called  $G_s$  and  $G_{olf}$  which stimulate adenylyl cyclase; and therefore, increases cAMP levels.  $A_{2A}$  receptors are primarily expressed in the striatum (Fredholm, Chen, Masino, & Vaugeois, 2005), but they are also found in blood vessels to exert a vasodilator effect in the brain and its periphery (Shi et al., 2008).  $A_{2B}$  receptor is coupled to  $G_s$  and activates adenylyl cyclase and phospholipase C (PLC), but it is at medium or low abundance. Likewise,  $A_3$  receptor activates PLC, but it is coupled to  $G_i$  that inhibits adenylyl cyclase. This receptor also increases intracellular  $Ca^{2+}$  levels upon activation (Dunwiddie & Masino, 2001).

Adenosine signaling is not only regulated by the action of receptors but also adenosine levels. Adenosine concentration is determined by the activity of intracellular and extracellular enzymes as well as adenosine transporters. Under stress conditions, dephosphorylation of adenosine triphosphate (ATP) is triggered, which further leads to adenosine monophosphate (AMP) formation. Next, 5'-nucleotidase converts AMP to adenosine, which is released outside the cell by nucleoside transporters, especially by equilibrative nucleoside

transporters (ENT) (King, Ackley, Cass, Young, & Baldwin, 2006). ATP can also be converted to adenosine by the action of several ectonucleases (Dunwiddie & Masino, 2001). Upon stress conditions like hypoxia, trauma, seizures and ischemia; a dramatic increase in extracellular adenosine concentrations occurs (Ribeiro, 2005).

**Table 1.1** Summary of adenosine receptor subtypes, their transduction pathways and main distributions in the brain (G: guanine nucleotide binding protein; AC: adenylate cyclase; GIRK: G-protein gated inward rectifying potassium channels; PLA2: phospholipase A2; PLD: phospholipase D; PLC: phospholipase C) (adapted from (Benarroch, 2008))

Receptor	G-protein coupling	Transduction pathway	Main distribution
A <sub>1</sub>	G <sub>i</sub> , G <sub>o</sub>	Inhibition of AC	Cerebral cortex
		N and P/Q channels inhibition	Hippocampus
		GIRK activation	Thalamus
		Activation of PLA2 and PLD	Cerebellum
			Brain stem
A <sub>2A</sub>	G <sub>s</sub> , G <sub>olf</sub>	Activation of AC	Spinal cord
			Striatum
A <sub>2B</sub>	G <sub>s</sub>	Activation of AC, PLC activation	Uniform at medium or low abundance
A <sub>3</sub>	G <sub>s</sub>	Activation of AC, PLC activation	Hippocampus and cerebellum at medium or low abundance

### **1.1.2.1 Adenosine A<sub>2A</sub> Receptor**

Adenosine A<sub>2A</sub> receptor is coupled to G<sub>s</sub> and G<sub>olf</sub>; thus, it stimulates AC and increases cAMP levels upon activation with an agonist (Fredholm, et al., 2005). Crystal structure of human A<sub>2A</sub> receptor has been determined with a 2.6 Angstrom level of resolution and in complex with an antagonist (Jaakola et al., 2008). This receptor subtype may be found as homo- or hetero-dimers with other G-protein coupled receptors. Their main localization in the central nervous system is striatum (Fredholm, et al., 2005). Apart from striatum, A<sub>2A</sub> receptors are also present in blood vessels (Shi, et al., 2008), microglia and astrocytes (Schwarzschild, Agnati, Fuxe, Chen, & Morelli, 2006). In the presynaptic region, A<sub>2A</sub> receptor activity has an antagonistic effect on inhibition of glutamate release from axon terminals by A<sub>1</sub> receptor activity in brain stem, cerebral cortex and striatum (Ribeiro, 2005). A<sub>2A</sub> receptor signaling in microvessels displays protective effects during ischemia or seizures by eliciting cerebral vasodilation. In astrocytes, A<sub>2A</sub> receptors signal to increase proliferation and activation of cells in the case of acute injury. In addition, astrocytic A<sub>2A</sub> receptors inhibit nitric oxide production, which, in turn, brings about neuroprotection. In microglial cells, A<sub>2A</sub> receptor activation induces neural growth factor release and serves as a neuroprotector. This receptor subtype has also anti-inflammatory effects by increasing IL-6 and IL-12 and infiltrating cells (Benarroch, 2008).

### **1.2 Interaction of Adenosine A<sub>2A</sub> and Dopamine D<sub>2</sub> Receptors**

Both of the adenosine A<sub>2A</sub> and dopamine D<sub>2</sub> receptors localize densely in the striatopallidal  $\gamma$ -aminobutyric acid (GABA) containing neurons (Ferre et al., 2004). These types of neurons are involved in the function of basal ganglia; therefore, have roles in disorders such as Parkinson disease and drug abuse

(Ferre, Fredholm, Morelli, Popoli, & Fuxe, 1997). This is why both receptors have been considered as main drug targets against psychiatric disorders, namely, Parkinson disease and schizophrenia (Ferre, et al., 2004). Early microdialysis and electrophysiology experiments have revealed that  $A_{2A}$  receptor activation shows an excitatory effect on striatopallidal neurons whereas  $D_2$  activation has an inhibitory effect. This result was an early proof of antagonistic functional interaction between  $A_{2A}$  and  $D_2$  receptors in basal ganglia (Ferre, et al., 1997). In the following years, animal studies show that  $A_{2A}$  antagonists potentiate antiparkinsonian effects of dopamine analogs (Bara-Jimenez et al., 2003). Also, it has been reported that stimulation of  $A_{2A}R$  decreases affinity of  $D_2R$  to its agonists (Ferre, von Euler, Johansson, Fredholm, & Fuxe, 1991). Another functional interaction example could come from the stimulation of adenylyl cyclase. As stated before,  $D_2R$  activation inhibits adenylyl cyclase, so decreases cAMP levels, which are increased by  $A_{2A}$  thorough  $G_{s/olf}$  coupling (Hillion et al., 2002). Hillion and colleagues also demonstrated co-immunoprecipitation, co-aggregation and co-internalization of  $D_2$  and  $A_{2A}$  receptors in cell lines transfected with both receptors (Hillion, et al., 2002). All of these findings have been raising the issue of direct protein-protein interaction between two receptors.

### **1.3 Dimerization of G-Protein Coupled Receptors**

Recent findings of studies with different GPCRs demonstrated that most G-protein coupled receptors form oligomers, either with themselves (homo-oligomers) or with other GPCRs (hetero-oligomers) (Park, Filipek, Wells, & Palczewski, 2004). Though there are several results supporting the hypothesis that GPCR dimers constitute the basic units for signaling, there are others proposing that GPCR dimers are necessary for passing quality control points during biosynthesis, maturation and trafficking to the membrane (Bulenger,

Marullo, & Bouvier, 2005). The most convincing proof for GPCR dimerization came from an atomic force microscopy study to demonstrate rhodopsin homodimers (Fotiadis et al., 2003). Other proofs have been provided with fluorescence and bioluminescence resonance energy transfer studies (Angers, Salahpour, & Bouvier, 2002). First GPCR heterodimer characterized was GABA<sub>B1</sub> and GABA<sub>B2</sub> obligate heterodimer. Experimental results have suggested that these two receptors have to be expressed in the same cell together to be expressed on the cell membrane at the normal, functional levels (Marshall, Jones, Kaupmann, & Bettler, 1999). Having observed dimerization of these GPCRs, scientists raise the question of why dimerization of these receptors occurs. There are various potential roles of GPCR dimerization. First is that GPCR may dimerize to provide 2:1 stoichiometry with the bound heterotrimeric G-protein. A study done with solution phase neutron scattering method proved that a leukotriene B<sub>4</sub> (BLT<sub>1</sub> receptor) dimer couples to one heterotrimeric G-protein in the presence of an agonist (Baneres & Parello, 2003). This study actually supports the hypothesis that one GPCR dimer may engage with only one G-protein. Another study illustrated that metabotropic glutamate (mGlu) receptor dimers can be partially activated if they are stimulated with one agonist; however, full activity can be gained by activating both protomers in the dimer (Kniazeff et al., 2004). This example supports a second hypothesis for the function of GPCR dimers; and this might be GPCRs may need to form dimers to get activated fully by the ligands. Beside functional roles, evidences for potential roles of GPCR dimerization in receptor biosynthesis and trafficking have been increasingly accumulated lately. This notion has gained power by the findings that many GPCRs start to dimerize early in the biosynthesis, in the ER; and their dimerization is constitutive, meaning that they do not necessarily get activated by agonists to dimerize (Bulenger, et al., 2005). For instance, C-C chemokine type 5 receptor (CCR5) forms constitutive oligomers; and these oligomers are neither enhanced nor inhibited by the effect of agonist introduction (Issafras et al., 2002). Likewise, constitutive homo- and

heterodimerization of oxytocin and vasopressin V1a and V2 receptors during biosynthesis have been experimentally shown (Terrillon et al., 2003). In addition, an HIV-1 co-receptor CXCR4, another GPCR, have also been reported to form homomultimers independent of the presence of ligands, existing as a constitutive oligomer (Babcock, Farzan, & Sodroski, 2003). All of the above mentioned examples indicate the requirement of some GPCRs to dimerize not for ligand dependent activation, but for biosynthesis and intracellular trafficking. Experimental data on receptor trafficking corroborate the idea of trafficking of a dimer to the plasma membrane together as a unit. For example, co-expression of  $\alpha_{1B}$ -adrenergic receptors increases cell surface expression of  $\alpha_{1D}$ -adrenergic receptors through heterodimerization (Hague, Uberti, Chen, Hall, & Minneman, 2004). Second interesting example for receptor trafficking is from olfactory receptor-  $\beta$ -adrenergic receptor dimerization. In heterologous expression studies, many failed to express olfactory receptors at the cell surface. However, in a study, it has been observed that co-expression of  $\beta_2$ -adrenergic receptor with mouse 71 (M71) olfactory receptor had a dramatic increasing effect on cell surface expression of the olfactory receptor (Hague et al., 2004). Dimerization of GPCRs happens to start in the ER, which is the organelle where the proteins are required to pass checkpoints for quality control.  $\beta_2$ -adrenergic receptor homodimerization can be given as an example for this phenomenon because this dimer has been found in the ER after cell-fractionation (Salahpour et al., 2004). Mutation studies also implicated the retention of non-dimerized receptors mostly in the ER, confirming the role of GPCR dimerization as an important strategy for trafficking to the cell surface. Several studies suggest that GPCR dimerization has an effect on agonist dependent receptor internalization. Ligand binding to only one protomer in the receptor heteromer may activate internalization of the dimeric unit as a whole. Examples of this type of endocytosis mechanisms come from SSTR<sub>1</sub> - SSTR<sub>5</sub> somatostatin,  $\delta$ -opoid -  $\beta_2$  adrenergic,  $\alpha_{2A}$  -  $\beta_1$  adrenergic, SSTR<sub>2A</sub> somatostatin  $\mu$ -opoid receptor heterodimers (reviewed in (Terrillon & Bouvier, 2004). As opposed to this

mechanism, heterodimerization of some GPCRs has an inhibitory effect on agonist driven endocytosis. To exemplify,  $\kappa$ -opoid receptor inhibits internalization of  $\delta$ -opoid receptors and  $\beta_2$  adrenergic receptors when they are heterodimerized with it (Jordan, Trapaidze, Gomes, Nivarthi, & Devi, 2001).

### **1.3.1 Methods to Detect Dimerization of G-protein Coupled Receptors**

There have been a variety of experimental approaches to detect dimerization of GPCRs and to study the pharmacological roles of it. These approaches mostly include co-immunoprecipitation (CoIP), resonance energy transfer techniques and functional complementation assays (Milligan & Bouvier, 2005). Of course, each technique has limitations beside their advantages. First, co-immunoprecipitation method was applied to detect homodimers of  $\beta_2$  adrenoreceptors in Sf9 insect cells. In this study, c-myc- and HA-tagged  $\beta_2$  adrenoreceptors were co-expressed and both types of receptors were detected in both anti-HA and anti-c-myc immunoprecipitates (Hebert et al., 1996). Another application of this technique is co-immunoprecipitation of GPCRs upon cross-linking via introduction of cysteine residues, which can form disulfide bonds, to the interaction sites to enhance dimerization. This technique has been used as an efficient tool to identify homodimerization of C5a receptors (Klco, Lassere, & Baranski, 2003). Despite its power to identify dimers, coimmunoprecipitation includes a tricky membrane preparation step. Unless fully soluble membrane fractions are produced with centrifugation at  $>100,000g$  for  $\sim 60$  minutes; or fractions are filtered through a  $0.22\mu m$  filter to ensure removal of insoluble fragments, coexpressed GPCRs may be detected after coimmunoprecipitation though they are not in actual physical contact (Milligan & Bouvier, 2005). Second, fluorescence resonance energy transfer (FRET) has been extensively utilized for dimerization studies. In one study, Overton and Blumer (2000) observed homodimers of yeast  $\alpha$ -factor receptor, Ste2 protein, with FRET

method in both membrane fractions and the whole yeast cells (Overton & Blumer, 2000). In another study, gonadotropin releasing hormone (GnRH) receptors have been shown to dimerize using FRET method; additionally, a dose dependent increase in FRET signal upon agonist introduction has been observed, pointing out agonist driven dimerization of GnRH receptors (Cornea, Janovick, Maya-Nunez, & Conn, 2001). In addition to FRET, bioluminescence resonance energy transfer (BRET), which depends on the energy transfer from the emission of a luciferase oxidated substrate to a fluorescent protein, became an alternative method for the detection of GPCR dimerization (Milligan, 2004b). Melatonin receptor 1 and 2 (MT1 and MT2) homodimerizations have initially been detected by means of BRET (Ayoub et al., 2002). As well as MT1 and MT2, homodimerization of  $\beta$ 2-adrenergic receptors have been reported to be detected in living cells using BRET technique (Angers et al., 2000). In the following years, better luciferase substrates and fluorescent proteins as acceptors have been utilized to increase the power and resolution of this assay (Milligan & Bouvier, 2005). Functional complementation assay can be listed as the third alternative technique to reveal GPCR dimers. This assay is based on the idea that there is a direct protein-protein interaction between two receptors provided that two types of nonfunctional GPCR mutants reconstitute receptor function or ligand binding when they are co-expressed. Angiotension AT1 receptor dimerization was firstly revealed using this method by co-expressing AT1 receptors with point mutations in transmembrane III and transmembrane V, neither of which can bind to the ligands. After co-expression of two AT1 receptor mutants, ligand binding ability of these receptors was reconstituted (Monnot et al., 1996).

### **1.3.1.1 Fluorescence (Förster) Resonance Energy Transfer**

Fluorescence (also known as Förster's) resonance energy transfer (FRET) is the non-radiative transfer of energy from an excited donor chromophore to an

acceptor chromophore, resulting in an energy emission from the acceptor (Förster, 1946). For FRET phenomenon to occur, firstly, the emission spectrum of the donor molecule should overlap with the excitation of the acceptor molecule. Secondly, donor and acceptor chromophores must be apart from each other with a distance no less than 100 Å (Milligan, 2004a). The efficiency of FRET (E) decreases with the 6<sup>th</sup> power of the distance between donor and acceptor molecules according to the following formula (Förster, 1946):

$$k_T = \left( \frac{1}{\tau_D} \right) \times \left( \frac{R_0}{R} \right)^6$$

$k_T$  being the rate of dipole-dipole transfer;  $\tau_D$  being the fluorescence lifetime of the donor;  $R$  being the distance between the donor and the acceptor; and  $R_0$  being the Förster distance where 50% of maximum FRET efficiency is yielded for the chosen FRET pair.

After the discovery of Green Fluorescent Protein (GFP) from the jelly fish *Victoria aequorea* (Shimomura, Johnson, & Saiga, 1962), it has been extensively used in cell biology to monitor the proteins by tagging fluorescent protein gene in frame with target protein's gene. This type of fusion proteins constructed with GFP and its differently colored derivatives have also been utilized in FRET studies (Tsien, 1998). In the early years, cyan fluorescent protein (CFP) and yellow fluorescent protein (YFP) was used as a FRET pair, also particularly for the detection of dimerization of GPCRs (Milligan & Bouvier, 2005). CFP and YFP tagged yeast Ste2 receptors were detected to be dimerizing with a FRET study (Overton & Blumer, 2000). In the later years, GFP and red fluorescent proteins were chosen to be better FRET pairs. To exemplify, this type of a FRET pair was chosen in a study for the dimerization of GnRH receptors (Cornea, et al., 2001).

Advantages of FRET over other methods are numerous. Firstly, FRET is capable of detecting interaction of protein in intact living cells. Secondly, it is a visual technique to detect subcellular localization of protein interactions (Herrick-Davis, Grinde, & Mazurkiewicz, 2004). Additionally, it is readily applicable for membrane proteins unlike other methods.

One of the best FRET pair of fluorescent proteins are now considered to be mCherry (a red fluorescent protein) – EGFP (enhanced GFP) because they present a suitable spectral overlap region for FRET studies, and there is a low level of crosstalk between excitation and emission spectra of mCherry and EGFP (Albertazzi, Arosio, Marchetti, Ricci, & Beltram, 2009).

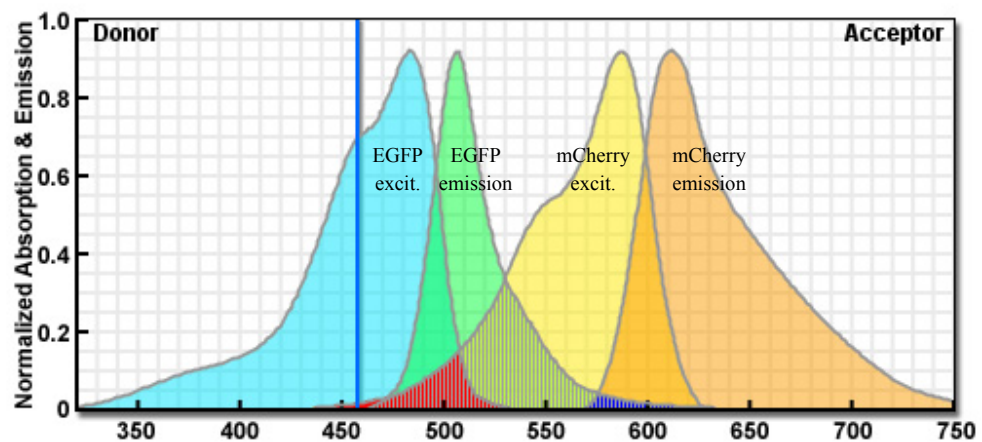


**Figure 1.4** Spectroscopic characteristics of EGFP (cyan-green) and mCherry (yellow-orange) (drawn with FRET for Fluorescent Proteins JAVA Tutorial provided by MicroscopyU of Nikon®)

As stated before, a suitable FRET pair should have a narrow emission overlap region. It is seen on Figure 1.2 that EGFP and mCherry pair is very convenient in this regard since they share the blue shaded part on the spectrum as the overlapping emission region of EGFP and mCherry, which is very narrow. Additionally, overlapping region of the excitation spectra of an ideal FRET pair should be very narrow as well. Exciting this pair at 458 nm (blue line on Fig. 1.2) can excite EGFP, but not mCherry, thereby allowing FRET between this pair by eliminating the possibility of direct excitation of acceptor, mCherry in this case. Lastly, emission spectrum of the donor and excitation spectrum of the acceptor should have a large overlapping region for energy transfer to be as easy as possible. On Figure 1.2, shaded area in all colors represents this overlap and it is seen to be large enough for FRET. All these criteria prove EGFP and mCherry to be a suitable FRET pair.

#### **1.4 Aim of the Study**

Adenosine  $A_{2A}$  and dopamine  $D_2$  receptors both affect neurophysiological events and are targeted by neuropsychiatric drugs. Thus, their physical interaction and mechanism of this interaction may reveal new ways to explain both physiology and pharmacology of these receptors in more detail as well as to pharmacologically target them more efficiently.

Therefore, this study aims optimizing FRET, as a powerful tool, to detect the heterodimerization of adenosine  $A_{2A}$  and dopamine  $D_2$  receptors, both being GPCRs. The strategy for this is, firstly, to develop reciprocal FRET pairs by tagging both  $D_2R$  and  $A_{2A}R$  with EGFP and mCherry fluorescent proteins. Secondly, these fluorescently labeled receptors will be transfected to live cells and visualized with laser scanning confocal microscope. Development of this fluorescence based live cell model will allow further studies to investigate the drugs or conditions that enhance or disturb the interaction of these receptors; and

thus their signaling pathways. Also, this live cell system can be used for high-throughput drug-screening studies for candidate anti-psychotics and other chemicals targeted to neurophysiological disorders.

## CHAPTER II

### MATERIALS & METHODS

#### 2.1 Materials

##### 2.1.1 Neuro2a (N2a) Mouse Neuroblastoma Cell Line and Media

Neuro2a cell line was used to express fluorescent protein tagged receptors via transient transfection. This cell line was directly purchased from ATCC; and kindly gifted by Assist. Prof. Dr. Tülin Yanık from METU Biological Sciences, Ankara, Turkey.

Dulbecco's Modified Eagle Medium (D-MEM) with L-glutamine (Invitrogen, Cat#41966029) together with OptiMEM<sup>®</sup>I Reduced Serum Medium with L-glutamine (Invitrogen, Cat#31985047) was used to grow N2a cells. Compositions of these media were tabulated in Appendix B. D-MEM and OptiMEM<sup>®</sup>I media were mixed 50:50; and they were added 10% Fetal Bovine Serum (Invitrogen, Cat#26140-079) and 5% Penicillin/Streptomycin solution (Invitrogen, Cat#15140-122). Final mixture was filtrated through Millipore Stericup<sup>®</sup> Filter Units in order to further sterilize it.

Dulbecco's Phosphate Buffered Saline (D-PBS) powder (Invitrogen, 21300-058) was dissolved in distilled, sterile water and used to wash cells in order to remove waste materials and dead cells over the cell layer. TrypLE<sup>™</sup> Express Stable Trypsin-Like Enzyme with Phenol Red (Invitrogen, Cat#12605-028) was

applied on cells to detach them from the bottom surface of the culture flask during passages.

N2a cells reach to 90% confluency in about 72 hours; therefore, they were subcultured at every three days by transferring 1/10<sup>th</sup> of cells into a 14 ml fresh growth medium containing T-75 flask.

Cells were frozen in freezing medium containing 35% D-MEM, 35% OptiMEM<sup>®</sup>1, 20% glycerol (as cryoprotectant) and 10% FBS. To freeze the cells, ~10<sup>7</sup> cells were centrifuged at 1000 rpm for 5 minutes. The cell precipitate was resuspended in 1 ml freezing medium and transferred to a screw-cap cryovial. These cryovials were stored in a -80°C freezer. After 24 hours, they were transferred to a liquid nitrogen tank to store them at around -150°C. To thaw frozen cells, cryovials were incubated at room temperature and the content was transferred into a fresh medium containing cell culture flask.

All of the chemicals and reagents used for cell culture were cell culture grade.

### **2.1.2 Neuro2a Cell Culture Conditions**

N2a cells were incubated at 37°C with 5% CO<sub>2</sub> in Heraeus<sup>®</sup> Hera Cell 150 Tri-Gas Cell Culture incubator. Cell culture studies were carried out in a laminar flow cabinet with a hepa filter.

### **2.1.3 Bacterial Culture Media and Conditions**

Luria Bertani (LB) medium was prepared to grow *Escherichia coli* TOP10 and XL1Blue cells. Composition of LB was given in Appendix C. Medium ingredients were dissolved in distilled water and pH was adjusted to 7.0 by adding 1N NaOH drop wise. After that, LB medium was sterilized by

autoclaving at 121°C for 20 minutes. For bacterial selection purposes, LB medium was supplemented with either 100 mg/mL ampicillin or 50 mg/mL kanamycin after cooling the medium down upon autoclaving.

Bacterial cultures were grown in both solid LB agar (containing additionally 1.5% agar) and liquid LB. Solid cultures were incubated at 37°C in a Nüve<sup>®</sup> brand incubator. However, liquid cultures were grown in a Zheiheng shaker incubator at 37°C. To prepare frozen bacterial stocks, an aliquot of culture in a liquid LB medium was mixed 50:50 with 50% glycerol to obtain 25% final glycerol concentration. This aliquot was stored at -80°C as a stock.

#### **2.1.4 Other Chemicals and Materials**

The chemicals utilized in this study were purchased from Sigma Chemical Company (NY, USA) and Applichem (Darmstadt, Germany). Molecular biology kits were from Fermentas (Ontario, Canada), QIAGEN (Düsseldorf, Germany) or Invitrogen (CA, USA). DNA polymerases used in polymerase chain reactions (PCR) were from Fermentas (Ontario, Canada) or Finnzymes (Vantaa, Finland). Restriction enzymes and DNA ligases were from New England Biolabs (Hertfordshire, UK). Cell culture media and reagents were all from GIBCO<sup>®</sup>, Invitrogen (CA, USA).

T-75 cell culture flasks were purchased from Greiner (Frankfurt, Germany). Sterile serological pipettes were from LP Italiana (Milano, Italy). Glass bottom dishes used for transfection and live cell imaging experiments were ordered from In Vitro Scientific (CA, USA).

All primer sets used in this study was synthesized by Alpha DNA (Quebec, Canada). Receptor cDNA clones were obtained from PlasmID, Harvard Medical School (MA, USA). Enhanced Green Fluorescent Protein (EGFP) and mCherry

cDNA vectors were kindly gifted by Prof. Dr. Henry Lester of California Institute of Technology (CA, USA).

Live cell imaging experiments were done with Leica LSM 510 laser scanning microscope.

## **2.2 Methods**

### **2.2.1 Preparation of Competent *E. coli* Cells by CaCl<sub>2</sub> Method**

An inoculum from *E. coli* stock was streaked onto an LB agar plate and incubated overnight at 37°C. Next day, a single cell was picked and inoculated into 5ml liquid LB medium and grown overnight at 37°C in the shaker incubator. The following day, 5 ml inoculum was transferred to a 50 ml LB medium containing 250 ml Erlenmeyer flask and incubated for 3 hours in the shaker incubator adjusted to 37°C. After the bacteria were grown for three hours, Erlenmeyer flask was chilled on ice for 15 minutes. Bacterial medium in the Erlenmeyer flask was transferred to a 50ml falcon tube; and centrifuged at 4000 rpm for 10 minutes. Supernatant was decanted and the pellet was resuspended with 15ml, sterile 0.1M CaCl<sub>2</sub> solution. This bacterial solution was chilled on ice for 15 minutes, and then centrifuged at 4000 rpm for 10 minutes. Supernatant was decanted and the pellet was resuspended with 4 ml, 0.1 M sterile CaCl<sub>2</sub> + 15% glycerol solution. At the final step, 100 µl aliquots in 1.5ml eppendorf tubes were prepared from this suspension; and they were stored in the -80°C freezer for further use in the next days.

### **2.2.2 Transformation of Competent *E. coli* cells with a plasmid**

Previously prepared competent *E. coli* cells were taken from the freezer and chilled on ice for 10 minutes to let them defreeze. 50-100 ng of plasmid

containing solution was added onto the competent cells. They were, in turn, incubated in ice for 30 minutes. At the next step, cells were applied a heat shock at 42°C for 90 seconds using a heat block. Then, the cells were directly transferred to ice to be chilled for 5 minutes. After that, 900 µl of sterile liquid LB was added onto the cells; and they were incubated at 37°C for 1 hour, but the tube was inverted at every 10 minutes not to let the cells precipitate. After 1 hour incubation, the cells were centrifuged at 10,000 rpm for 1 minute. 900 µl of the supernatant was discarded. Cells in the pellet were resuspended in 100 µl of the supernatant and inoculated onto LB agar plate containing the corresponding antibiotic, which the plasmid carries resistance against, using glass beads. Agar plates were incubated in 37°C incubator.

After transformation, a single colony grown on the LB agar plate with antibiotic resistance was picked and inoculated to 4 ml liquid LB broth to grow overnight at 37°C. The next day, 4 ml bacterial inoculum was used to isolate plasmid with Fermentas® GeneJET™ Plasmid Miniprep Kit according to instructor's manual.

### **2.2.3 Restriction Enzyme Digestion**

All restriction enzymes used in the course of this thesis work were purchased from New England Biolabs Inc. (NEB), thus, all digestion reactions were done according to supplier's suggestions. 1 µg of plasmid DNA or PCR product was digested with 1 unit of the restriction enzyme in the provided NEB buffer (Appendix D) diluted to 1X. Whenever suggested, 1X BSA was added to digestion reaction. After the mixture was prepared, it was incubated at 37°C for 2 hours.

## 2.2.4 Ligation

Digested products and plasmids were ligated *in vitro* using T4 DNA ligase (NEB, Cat#0202T) in 1X T4 DNA ligase buffer (Appendix D) provided by NEB. For ligation, 1:5 vector to insert ratio was used; and amounts of vector and insert were calculated accordingly, considering their sizes as well.

## 2.2.5 Polymerase Chain Reaction (PCR)

To amplify fluorescent protein genes with 30 bp overhangs, which would be necessary for PCR integration protocol, the following optimized PCR protocol was applied.

**Table 2.1** Optimized PCR conditions to amplify fluorescent protein coding sequences, mCherry (Accession Number: ACO48282, 708bp) and EGFP (Accession Number: AAB02574, 720bp)

Reagent	Volume	
Nuclease free water	38.3 $\mu$ l	
Taq Buffer (10X)	5 $\mu$ l	94°C for 5 min
MgCl <sub>2</sub>	3 $\mu$ l	94°C for 30 sec
dNTP (25mM)	0.5 $\mu$ l	53°C for 45 sec
Forward primer (20 pmol)	1 $\mu$ l	72°C for 1min
Reverse primer (20 pmol)	1 $\mu$ l	72°C for 5 min
Template	1 $\mu$ l	
Taq DNA Polymerase	0.2 $\mu$ l	
<b>Total</b>	<b>50 <math>\mu</math>l</b>	

} 35 cycles

### **2.2.6 Agarose Gel Electrophoresis**

To check the sizes of PCR products and further gel extraction procedures, agarose gel electrophoresis was carried out. 1% w/v agarose gel was prepared and used throughout the experiments. The gel was run in 1X TBE (Appendix D) at 100V for about 30-35 minutes. For each gel electrophoresis experiment, one lane was loaded with an appropriate DNA size ladder. DNA sample to be loaded onto agarose gel was mixed with 6X DNA loading dye (Fermentas®, Cat#R0611, see Appendix D) with 5:1 DNA to loading dye ratio to get 1X loading dye concentration at the end.

### **2.2.7 Extraction of DNA from Agarose Gel**

To extract PCR and/or digestion products from agarose gel after electrophoresis, QIAGEN® Gel Extraction Kit (Cat# 28704) was used. After the desired band was excised on the UV plate, the following procedure was the same as given in the instruction guide of the kit.

### **2.2.8 Quantification of DNA Amount**

To quantify the amount of DNA after plasmid isolation and gel extraction protocols, NanoDrop 2000 spectrophotometer from Thermo Scientific® was utilized. 1.5 µl of the sample solution was loaded onto the micro-volume pedestal and the measurement was done as directed by user's manual.

### **2.2.9 PCR Integration Method**

To tag receptors with fluorescent proteins at their C-termini, PCR integration method was applied. This method involves two tandem PCR reactions where, in the first PCR reaction, fluorescent protein genes had been amplified with 30 bp

overhangs determined by the target location. For this, the last 30 bp of the receptor gene without the stop codon was added at the 5' of the forward primer; on the other hand, there was the 30 bp of the vector (pcDNA 3.1 (-)) sequence that directly follows the receptor gene sequence at the 5' of the reverse primer. The double stranded PCR product of this first reaction was used as the primer set in the PCR integration reaction. As template, pcDNA 3.1 (-) eukaryotic expression vector carrying either A<sub>2A</sub> or D<sub>2</sub> receptor gene was used; its amount was 1/5<sup>th</sup> of the PCR product from the first PCR reaction. With this second PCR, a new full vector with fusion receptor gene was amplified. To be able to make this amplification possible, a high fidelity DNA polymerase, Phire<sup>®</sup> Hot Start DNA Polymerase was used. The above mentioned experimental strategy was illustrated in Figure 2.1.

**Table 2.2** Conditions for PCR integration method to produce receptors tagged with a fluorescent protein

<b>Reagent</b>	<b>Volume/Amount</b>
Phire <sup>®</sup> Reaction Buffer (5X)	10 µl
dNTP (25mM)	1 µl
1st PCR product	500ng
Template	100ng
Phire <sup>®</sup> DNA Polymerase	1 µl
Nuclease free water	Required volume to complete up to 50 µl
<b>Total</b>	<b>50 µl</b>

95°C for 30 sec  
 → 95°C for 30 sec  
 → 51°C for 1 min  
 → 68°C for 2 min/kb

} 18 cycles

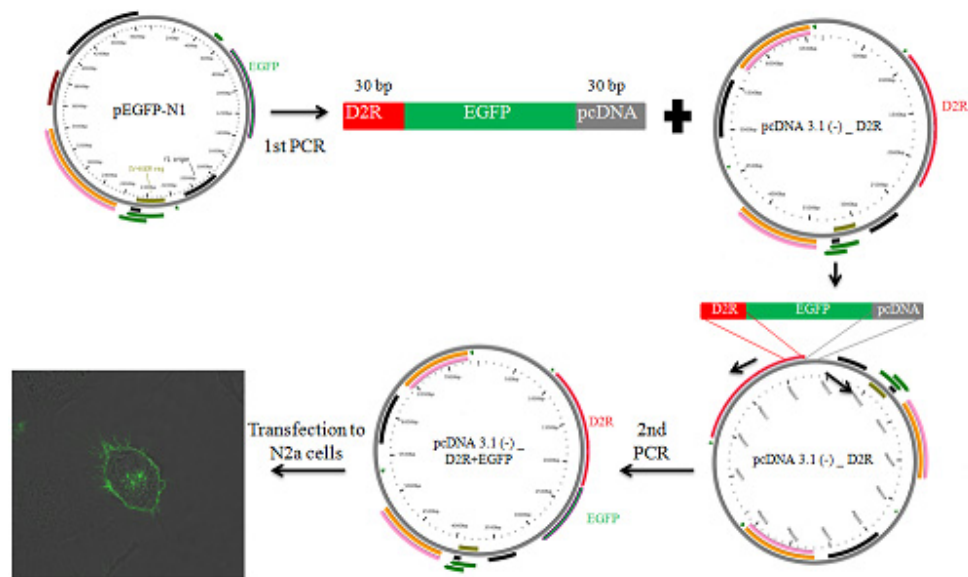


**Figure 2.1** Experimental strategies outlining the methods of designing fluorescently tagged receptors (tagging D<sub>2</sub>R with EGFP was given here as a representative of all constructs)

### 2.2.10 Transfection of N2a cells with pcDNA 3.1 (-) eukaryotic expression vector

For eukaryotic transfection, Lipofectamine<sup>TM</sup> LTX with Plus<sup>TM</sup> reagents from Invitrogen<sup>®</sup> was used. At the first day, 100,000 N2a cells were seeded on a glass bottom dish by adding 2 ml of OptiMEM<sup>®</sup> I, reduced serum free medium. After letting cells grow for 24 hours, transfection protocol was started the next day. 500 ng of the desired plasmid was diluted in 100  $\mu$ l of OptiMEM<sup>®</sup> I and 6  $\mu$ l of Plus<sup>TM</sup> reagent was added to this mixture. The resultant mixture was incubated for 15 minutes at room temperature. Then, 4  $\mu$ l of Lipofectamine LTX<sup>TM</sup> was diluted with OptiMEM I in a separate tube; and this was added at the end of 15

minutes to the previously prepared plasmid DNA + Plus<sup>TM</sup> + OptiMEM<sup>®</sup> I mixture. The final transfection mixture was formed in this way; and this mixture was also incubated for 15 minutes at room temperature. Meanwhile, the medium on the cells were discarded and cells were rinsed with 1 ml of sterile PBS solution. After that, 1 ml of OptiMEM<sup>®</sup> I was added onto the cells. When 15 minute incubation of transfection mix was complete, it was added drop wise in the medium on the cells. The cells were incubated for 3 hours in the 5% CO<sub>2</sub> incubator at 37°C. At the end of 3 hours, 2.5 ml of normal growth medium containing serum was added onto the transfected cells. For double transfection, 500 ng of each plasmid was added to the transfection mixture.

#### **2.2.11 Imaging Transfected N2a Cells with Laser Scanning Confocal Microscope**

For each FRET analysis, three transfection reactions were done; with only donor (receptor + EGFP), with only acceptor (receptor + mCherry) and with both donor and acceptor constructs. The cells transfected with only donor construct were used to calculate how much of the fluorescence was involved in the donor bleed-through. In contrast, the cells transfected only with acceptor construct were used to calculate acceptor bleed-through. Double transfected construct was used in FRET setup.

For FRET analysis, double transfected cells were excited at 458 nm, which can excite EGFP, and the emission was collected over 585 nm, which comes from mCherry. Additionally, two more images from the same region of interest were taken for normalization of bleed-throughs. First image was taken after exciting the cells at 458 nm and emission was collected in the 505-580 nm range (EGFP channel). Second image was taken by exciting them at 543 nm for mCherry and emission was detected over 585 nm (mCherry channel). For donor bleed through calculations, cells transfected only with EGFP tagged receptors were

excited at 458 nm and detected at both EGFP and mCherry channels. For acceptor bleed-through computation, cells transfected with only mCherry tagged receptor were excited at 458 nm and 543 nm; both emissions were detected at mCherry channel. All FRET analyses were done by using PixFRET plug-in of ImageJ software (Feige, Sage, Wahli, Desvergne, & Gelman, 2005).

### **2.2.12 Image Analysis with Pix-FRET**

In FRET analysis, a very major problem is to calculate and normalize spectral bleed-throughs (SBTs), in other words, a false positive FRET signal that comes from excitation of the acceptor by donor laser or emission of the donor in acceptor channel. Pix-FRET contains an algorithm to overcome this problem.

To be able to use Pix-FRET, three sets should be prepared. The first set is for donor bleed-through and it involves only donor fluorophore. Two images from this set is taken with the following setups;

- excitation of the donor and emission of the acceptor
- excitation of the donor and emission of the donor

For acceptor bleed-through, only acceptor fluorophore should be present and two images should be taken with the following setups;

- excitation of the donor and emission of the acceptor
- excitation of the acceptor and emission of the acceptor

For FRET, two fluorophores must be present at the same time and three images are taken this time with the following configurations;

- excitation of the donor and emission of the acceptor
- excitation of the donor and emission of the donor
- excitation of the acceptor and emission of the acceptor

Using bleed-through images, Pix-FRET outputs three line equations; constant, linear and exponential; that fit and comprise most of the pixel intensity values.

The best line from these is chosen to normalize the bleed-through. Afterwards, FRET image is analyzed according to this normalization.

## CHAPTER III

### RESULTS & DISCUSSION

#### 3.1 Cloning of *DRD2* coding sequence from pDONR221 to pDNR-Dual vector

The cDNA of dopamine D<sub>2</sub> receptor gene was bought in pDONR221 (see Appendix E), which is a donor vector designed for gateway system. On the other hand, cDNA of adenosine A<sub>2A</sub> receptor was obtained in pDNR-Dual (see Appendix E) vector between *SalI* and *HindIII* restriction enzyme sites. To have both receptors in the same vector and continue the further procedures using just one vector, *DRD2* coding sequence was cloned to pDNR-Dual vector. The strategy was to amplify *DRD2* coding sequence with restriction enzyme (RE) sites, digest the ends of PCR product and ligate to pDNR-Dual vector. For this, *SalI* restriction enzyme cut site was added to 5' of the forward primer; and *HindIII* cut site was added to 5' of the reverse primer. The primers are listed in Appendix G.

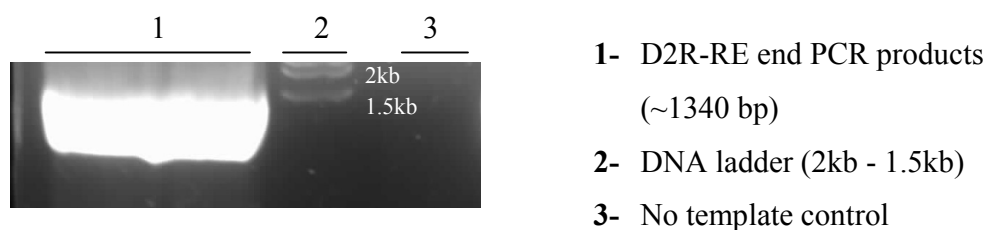


**Figure 3.1** PCR product of *DRD2* cDNA with RE ends run on 1% agarose gel

This PCR product was excised from the gel shown on Fig. 3.1; and eluted using gel extraction kit. Gel eluted PCR product and pDNR-Dual vector carrying A<sub>2A</sub>R cDNA was digested with *SalI* and *HindIII* sequentially.

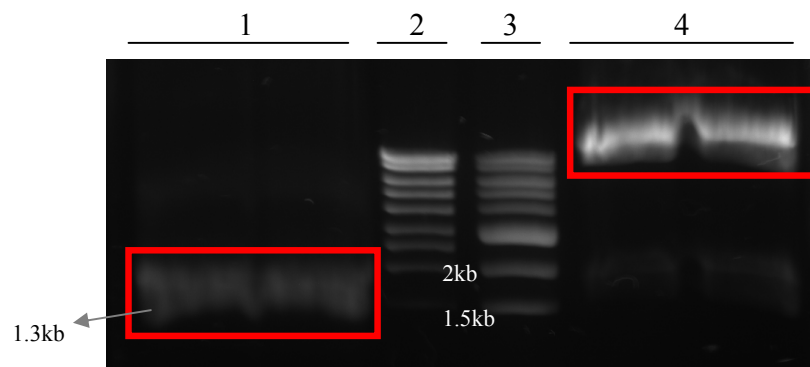


**Figure 3.2** *SalI* and *HindIII* digestion products of D<sub>2</sub>R PCR product (lane 1) and pDNR-Dual\_A<sub>2A</sub>R vector (lane 4). Lane 2 was loaded with Fermentas® High range mass ruler and lane 3 was loaded with NEB 1 kb ladder

On Fig. 3.2, D<sub>2</sub>R coding sequence amplified and digested with REs is seen on the lane 1, in the red box. On lane 4, digested pDNR-Dual vector is seen on the upper part of the gel, in the red box. Below that, there is another band around 1.2 kb, which corresponds to A<sub>2A</sub>R gene. By looking at this gel photo, it is seen that pDNR-Dual was cut well and A<sub>2A</sub>R gene was dropped between *SalI* and *HindIII* cut sites on the vector. After that, these two bands in the red boxes were extracted from the gel with the kit and ligation reaction was set with D<sub>2</sub>R insert and pDNR-Dual empty vector. After 1 hour ligation, product was directly transformed to competent *E. coli* cells. Two colonies grown after this

transformation were inoculated to liquid LB and their plasmids were isolated. The plasmids were PCR amplified with D<sub>2</sub>R primers to confirm the presence of D<sub>2</sub>R insert in this new vector.

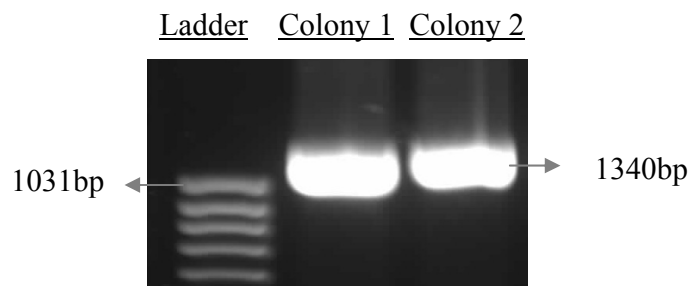


**Figure 3. 3** PCR to amplify D<sub>2</sub>R coding sequence from isolated plasmids of ligation of D<sub>2</sub>R to pDNR-Dual vector.

According to PCR result on Fig. 3.3, both colonies had D<sub>2</sub>R inserts in pDNR-Dual vector.

### **3.2 Tagging A<sub>2A</sub> Receptor with mCherry Using PCR Integration Method**

mCherry coding sequence (Accession Number: ACO48282, 708bp) was amplified from pCS2-mCherry vector using the primers to amplify mCherry cDNA with A<sub>2A</sub>R flanking ends (see Appendix G). Using these primers, mCherry coding sequence was PCR amplified and run on agarose gel as seen on Fig. 3.4.

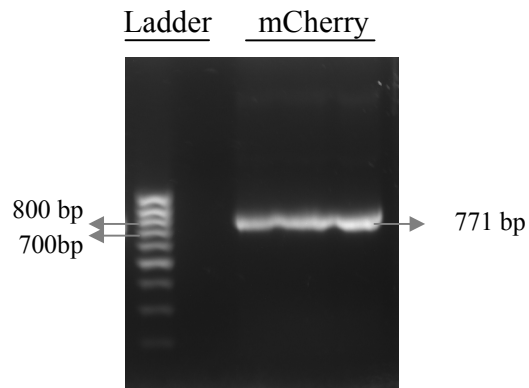
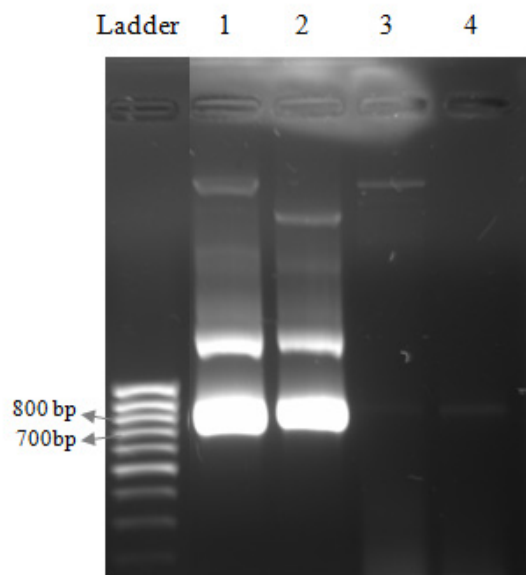


**Figure 3.4** Agarose gel electrophoresis photo of mCherry PCR amplification with A<sub>2A</sub> flanking ends

mCherry PCR product was extracted from the gel and used for PCR integration method as primers. The template of this PCR was pDNR-Dual\_A<sub>2A</sub>R. After this PCR reaction, product was a low concentrated full plasmid solution carrying A<sub>2A</sub>R + mCherry, so it was transformed to competent *E. coli* cells to increase the concentration of plasmids. Plasmids of two grown colonies after transformation were isolated and screened for the presence of the mCherry insert, which should be 771 bp. The gel is presented below on Fig. 3.5:



- 1- pDNR-Dual\_A<sub>2A</sub>R + mCherry
- 2- Positive control
- 3- pDNR-Dual\_A2A
- 4- No template control

**Figure 3.5** Agarose gel photo of PCR product of mCherry amplified from pDNR-Dual\_A<sub>2A</sub>R

Newly constructed pDNR Dual vector with A<sub>2A</sub>R-mCherry fusion was confirmed to be containing mCherry gene with PCR. The specificity of this PCR reaction was checked with positive and negative controls. To express this construct in N2a mammalian cell line, A<sub>2A</sub>R-mCherry fusion, which had been between *SalI* and *HindIII* sites on pDNR-Dual vector (see Fig. 3.6), was cut from this vector with *NotI* and *HindIII* and ligated to a mammalian expression vector pcDNA 3.1 (-) from the same sites after sequencing A<sub>2A</sub>R-mCherry region and confirming it to be correct.

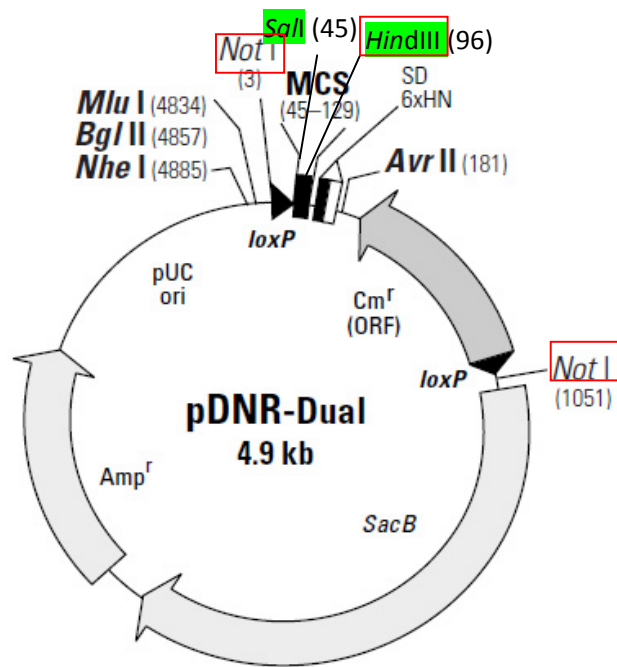


**Figure 3.6** Map of pDNR-Dual vector. Green RE sites represent those between which A<sub>2A</sub>R+mCherry insert is located; those in red boxes show where the insert is cut

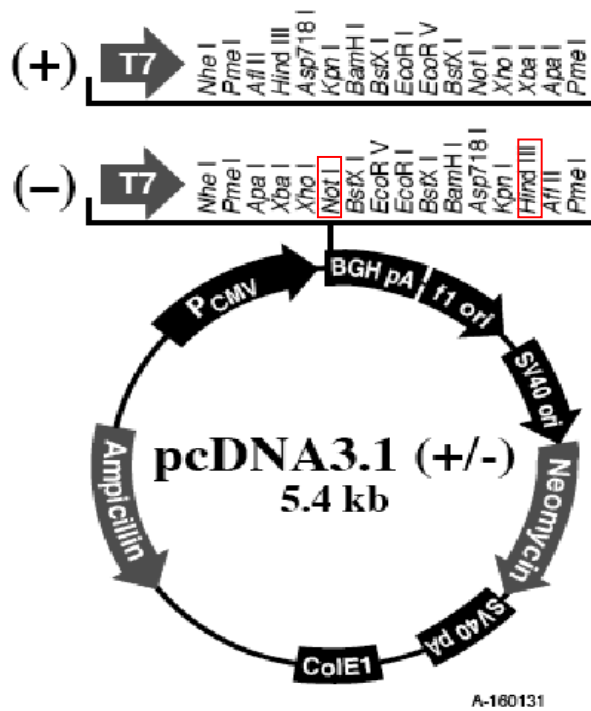


**Figure 3.7** Map of pcDNA 3.1 (-). RE sites in red boxes show where the A<sub>2A</sub>R + mCherry insert is ligated

pDNR Dual\_A2AR + mCherry and pcDNA 3.1 (-) vector, shown on Fig. 3.7, carrying a 2 kb insert between *NotI* and *HindIII* sites were digested in the same reaction.

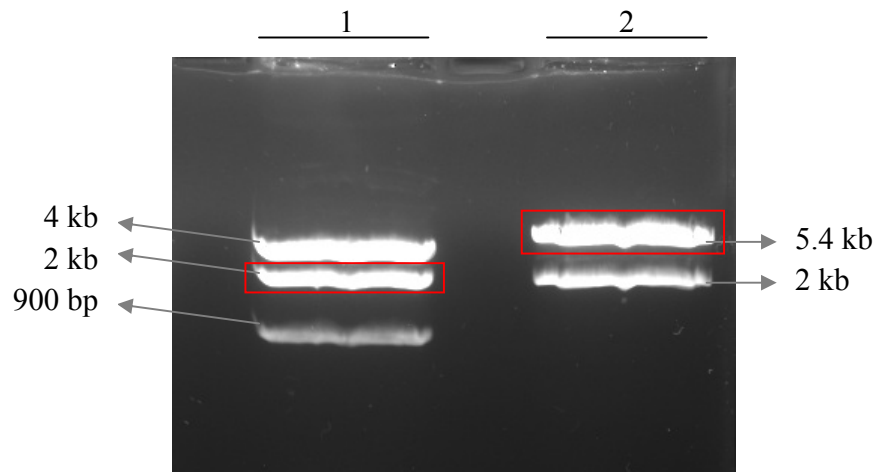


**Figure 3.8** *NotI* and *HindIII* digested pDNR-Dual\_A2AR + mCherry (lane 1) and pcDNA 3.1 (-) with a 2 kb insert (lane 2)

Digestion of pDNR-Dual\_A<sub>2A</sub>R + mCherry produced three fragments. 2 kb fragments belonged to A<sub>2A</sub>R + mCherry fusion gene as seen above on Fig 3.8. Other 4 kb and 900 bp fragments belonged to pDNR-Dual vector. The bands in the red boxes, namely, A<sub>2A</sub>R + mCherry insert and empty pcDNA 3.1 (-) were extracted from the gel and put into ligation reaction. Transformation proceeded ligation and positive colonies were chosen for plasmid isolation. These plasmids were screened with PCR for the presence of mCherry gene as a confirmation of successful ligation.

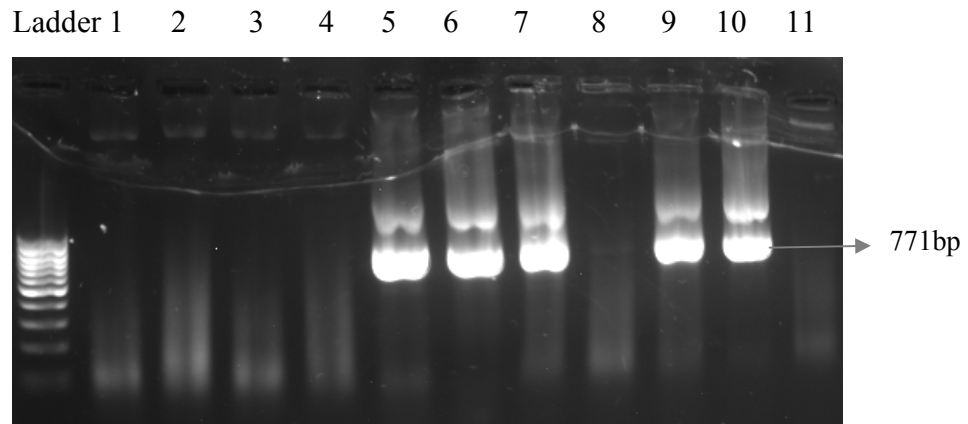


**Figure 3.9** Agarose gel photo of mCherry PCR to screen potential pcDNA 3.1 (-)<sub>A<sub>2A</sub>R</sub> + mCherry plasmids. Numbers 1-9 represent different colonies chosen from the plate. Lane 10 was loaded with a positive control. Lane 11 was loaded with empty pcDNA 3.1 (-).

As shown on Fig. 3.9, the colonies 5, 6, 7 and 9 had the ligated pcDNA 3.1 (-)<sub>A<sub>2A</sub>R</sub> + mCherry vector. These were also verified by digestion with *NotI* and *HindIII* to check the sizes of the inserts.

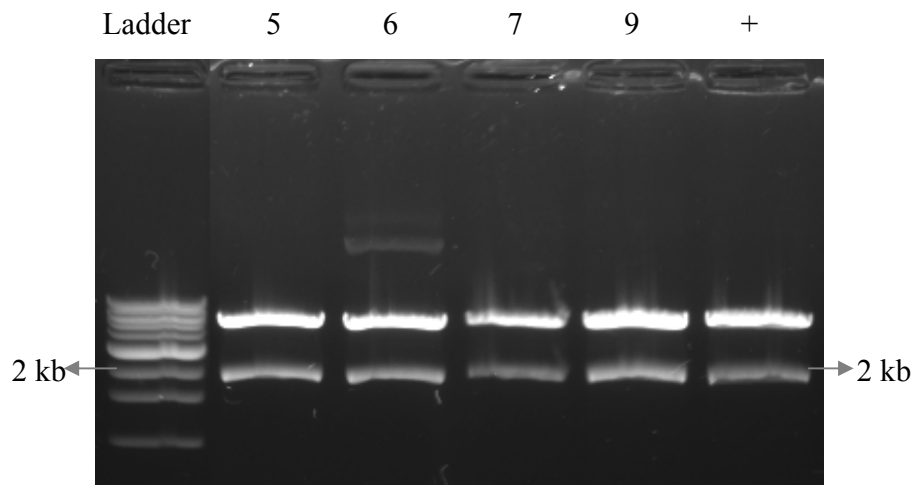


**Fig. 3.10** Agarose gel photo of NotI and HindIII double digested pcDNA 3.1 (-)  $A_{2A}R$  + mCherry. Lanes 5, 6, 7 and 9 represent the screened colonies; + represents the positive control.

The Fig. 3.10 shows that 5, 6, 7 and 9 had the inserts of the expected size, 2kb, which corresponds to the size of  $A_{2A}R$  + mCherry. To confirm whether the insert had also the expected sequence without any insertions, deletions or missense mutations, the plasmid 7 was sent for sequencing. The sequencing results confirmed that mCherry gene was successfully inserted to the end of  $A_{2A}R$  by eliminating the stop codon of  $A_{2A}R$ . The sequence of  $A_{2A}R$ +mCherry fusion coding sequence is given on Fig 3.11. Black sequence belongs to  $A_{2A}R$ , red sequence belongs to mCherry coding sequence. Highlighted parts show the locations where the forward sequencing primers are designed for. Apart from these, a reverse primer within the vector sequence following mCherry gene was also utilized to sequence this 2 kb region.

ATGCCATCATGGGCTCCTCGGTGTACATCACGGTGGAGCTGGCCATTGCTGTGCTGGCCATCC  
 TGGGCAATGTGCTGGTGTGCTGGGCCGTGTGGCTCAACAGCAACCTGCAGAACGTCAACCACTA  
 CTTTGTGGTGTCACTGGCGGCGGCCGACATCGCAGTGGGTGTGCTCGCCATCCCCTTTGCCATC  
 ACCATCAGCACCGGGTTCTGCGCTGCCTGCCACGGCTGCCTCTTCATTGCCTGCTTCGTCCTGG  
 TCCTCACGCAGAGCTCCATCTTCAGTCTCCTGGCCATCGCCATTGACCGTACATTGCCATCCG  
 CATCCCGCTCCGGTACAATGGCTTGGTGAACGGCAGAGGGCTAAGGGCATCATTGCCATCTGC  
 TGGGTGCTGTCGTTTGGCCATCGGCCTGACTCCCATGCTAGGTTGGAACAACCTGCGGTGAGCCAA  
 AGGAGGGCAAGAACCCTCCCAGGGCTGCGGGGAGGGCCAAGTGGCCTGTCTCTTTGAGGATGT  
 GGT**CCCCATGAACTACATGGTGTAC**TTCAACTTCTTTGCCTGTGTGCTGGTGCCCTGCTGCTC  
 ATGCTGGGTGTCTATTTGCGGATCTTCTGGCGGCGGACGACAGCTGAAGCAGATGGAGAGCC  
 AGCTCTGCCGGGGAGCGGGCACGGTCCACACTGCAGAAGGAGGTCCATGCTGCCAAGTCACT  
 GGCCATCATTGTGGGGCTCTTTGCCCTCTGCTGGCTGCCCTACACATCATCAACTGCTTCACT  
 TTCTTCTGCCCGACTGCAGCCACGCCCTCTCTGGCTCATGTACCTGGCCATCGTCTCTCCC  
 ACACCAATTCGGTTGTGAATCCCTTTCATCTACGCTACCGTATCCGCGAGTTCGCCAGACCTT  
 CCGCAAGATCATTTCAGCCACGTCCTGAGGCAGCAAGAACCTTCAAGGCAGTGGCACCAGT  
 GCCCGGTCTTGGCAGCTCATGGCAGTGACGGAGAGCAGGTCAGCCTCCGTCTCAACGGCCACC  
 CGCCAGGAGTGTGGGCCAACGGCAGTGCTCCCCACC**CTGAGCGGAGGCCCAATG**GCTACGCCCT  
 GGGCTGGTGTGAGTGGAGGGAGTGCCCAAGAGTCCCAGGGGAACACGGGCCTCCCAGACGTGGAG  
 CTCTTAGCCATGAGCTCAAGGGAGTGTGCCAGAGCCCCCTGGCCTAGATGACCCCTGGCCC  
 AGGATGGAGCAGGAGTGTCC**ATGGT**GAGCAAGGGCGAGGAGGATAACATGGCCATCATCAAGGA  
 GTTCATGCGCTTCAAGGTGCACATGGAGGGCTCCGTGAACGGCCACGAGTTCGAGATCGAGGGC  
 GAGGGCGAGGGCCGCCCTACGAGGGCACCCAGACCGCCAAGCTGAAGGTGACCAAGGGTGGCC  
 CCCTGCCCTTCGCCTGGGACATCCTGTCCCCTCAGTTCATGTACGGCTCCAAGGCCTACGTGAA  
 GCACCCCGCGACATCCCCGACTACTTGAAGCTGTCTTCCCCGAGGGCTTCAAGTGGGAGCGC  
 GTGATGAACTTCGAGGACGGCGGCGTGGTGAACCGTGAACCGAGGACTCCTCCCTGCAGGACGGCG  
 AGTTCATCTACAAGGTGAAGCTGCGCGGCACCAACTTCCCCTCCGACGGCCCCGTAATGCAGAA  
 GAAGACCATGGGCTGGGAGGCCTCCTCCGAGCGGATGTACCCCGAGGACGGCGCCCTGAAGGGC  
 GAGATCAAGCAGAGGCTGAAGCTGAAGGACGGCGGCCACTACGACGCTGAGGTCAAGACCACCT  
 ACAAGGCCAAGAAGCCCGTGCAGCTGCCCGGCGCCTACAACGTCAACATCAAGTTGGACATCAC  
 CTCCACAACGAGGACTACACCATCGTGAACAGTACGAACGCGCCGAGGGCCGCCACTCCACC  
 GCGGCATGGACGAGCTGTACAAGTAA

**Figure 3.11** Coding sequence of A<sub>2A</sub>R+mCherry fusion. Black sequence belongs to A<sub>2A</sub>R (Accession Number: NM\_000675), red sequence belongs to mCherry coding sequences (Accession Number: ACO48282). Highlighted parts show the locations where the forward sequencing primers are designed for.

After sequence confirmation, pcDNA 3.1 (-)<sub>A<sub>2A</sub>R</sub>+mCherry vector was transfected to cultured N2a cells and observed with laser scanning confocal microscope (Fig. 3.12). The cells were excited at 543 nm to excite mCherry near its excitation maximum; emission was collected over 585 nm.

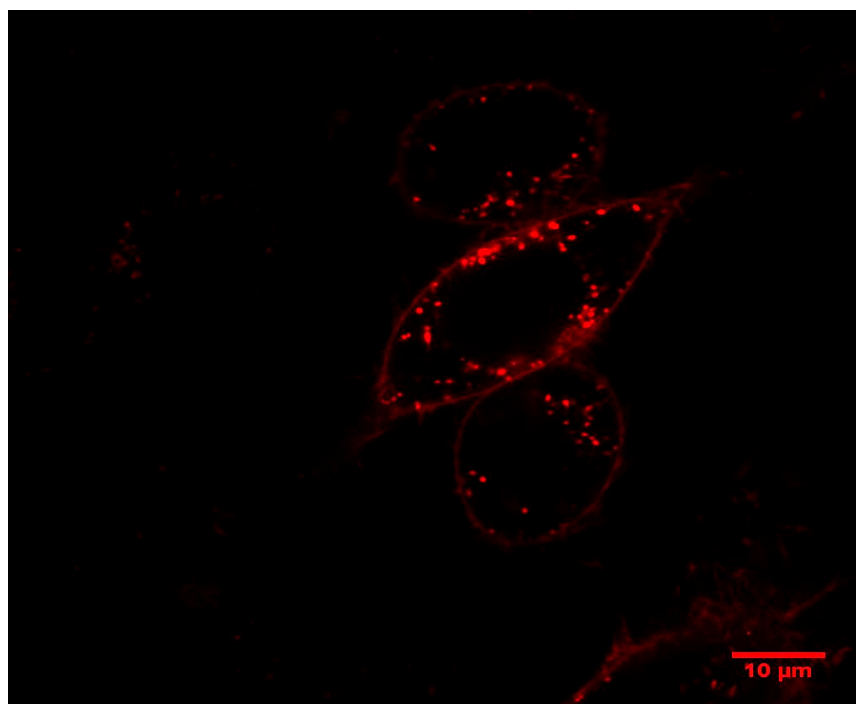


**Figure 3.12** N2a cells transfected with pcDNA 3.1 (-)<sub>A<sub>2A</sub>R</sub>+mCherry vector, excited at 543 nm

### 3.3 Cloning of A<sub>2A</sub>R and D<sub>2</sub>R cDNAs to pcDNA 3.1 (-) mammalian expression vector

To directly synthesize fusion constructs in the expression vector pcDNA 3.1(-), D<sub>2</sub>R and A<sub>2A</sub>R genes were cloned from pDNR-Dual to pcDNA 3.1(-). For this, pDNR-Dual\_A<sub>2A</sub>R and constructed pDNR-Dual\_D<sub>2</sub>R were cut from *NotI* and *HindIII* sites (see Fig3.13); and cloned to the same RE sites of pcDNA 3.1 (-).

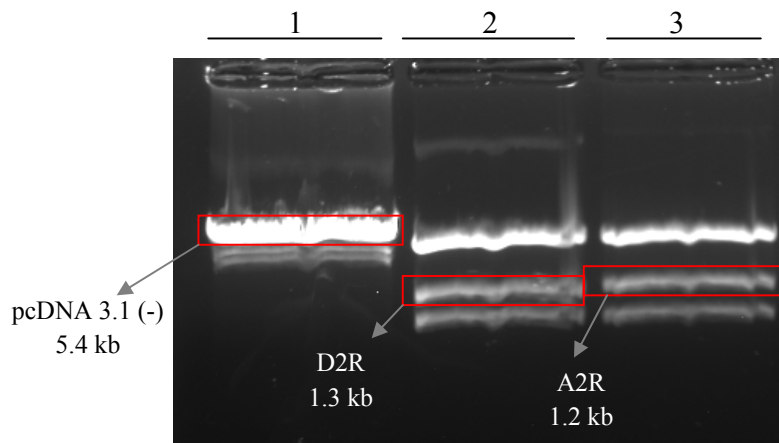


**Figure 3.13** pcDNA 3.1 (-) (lane 1), pDNR-Dual\_A<sub>2A</sub>R (lane 2) and pDNR-Dual\_D<sub>2</sub>R (lane 3) that were cut with *NotI* and *HindIII*

The bands in the red boxes, pcDNA 3.1(-), A<sub>2A</sub>R insert and D<sub>2</sub>R insert respectively, were excised and extracted from gel for further use in ligation. Consequently, transformation done after ligation yielded colonies; then, they were screened with digestion and size control. Size check for D<sub>2</sub>R insert with double digestion is seen on Fig. 3.14.

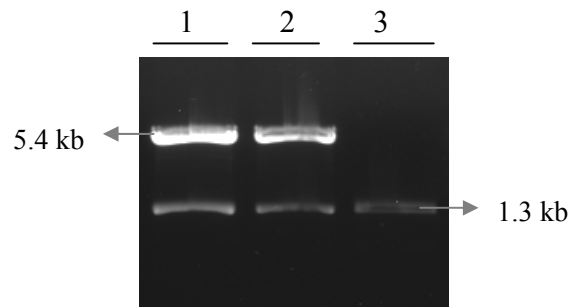


**Figure 3.14** pcDNA 3.1 (-)<sub>D2R</sub> plasmids (lane 1-2) digested with *NotI* and *HindIII* run on agarose gel electrophoresis together with D2R insert alone as positive control (lane 3)

The plasmids were also put into PCR reaction with D<sub>2</sub>R primers to check the presence of D<sub>2</sub>R insert. Agarose gel photo of PCR results is shown below on Fig. 3.15.

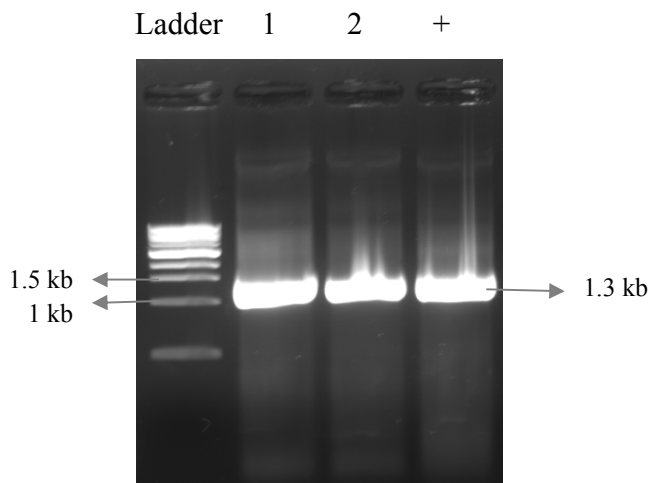


**Figure 3.15** Agarose gel photo of PCR products of pcDNA 3.1 (-)<sub>D2R</sub> plasmids. Lane 1 and 2 were loaded with plasmids #1 and #2, respectively. Lane + had pDONR 221\_*DRD2* vector that originally carried D<sub>2</sub>R coding sequence.

Digestion experiment and PCR to confirm the presence of D<sub>2</sub>R gene in the pcDNA 3.1 (-)<sub>D2R</sub> vectors confirmed these plasmids to be correctly ligated. Thus, they were used for further steps.

In another set of experiments, A<sub>2A</sub>R gene was ligated to pcDNA 3.1 (-) and the resultant plasmids were controlled with digestion and size control (Fig. 3.16).

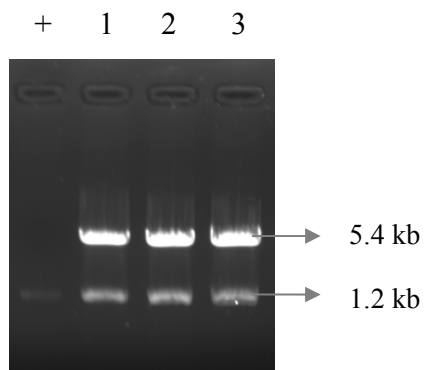


**Figure 3.16** Agarose gel photo of *NotI-HindIII* digestion products of pcDNA 3.1 (-)<sub>A<sub>2A</sub>R</sub> plasmids. Lane 1, 2 and 3 were loaded with digested plasmids #1, #2 and #3, respectively. Lane + had only A<sub>2A</sub>R insert.

Digestion control experiment showed that all three chosen plasmids have the desired A<sub>2A</sub>R insert. These plasmids were used in the further steps.

### **3.4 Tagging Dopamine D<sub>2</sub> Receptor with mCherry and EGFP Using PCR Integration Method**

EGFP coding sequence was amplified with the primers to obtain EGFP with flanking regions (see Appendix G). The same primers were used to amplify mCherry as well since both EGFP and mCherry coding sequences share the same primer annealing sequences.

EGFP gene was amplified from pEGFP-N1 vector; whereas, mCherry gene amplified from pCS2-mCherry vector. The photo of agarose gel loaded with the PCR products is seen on Fig. 3.17 below.

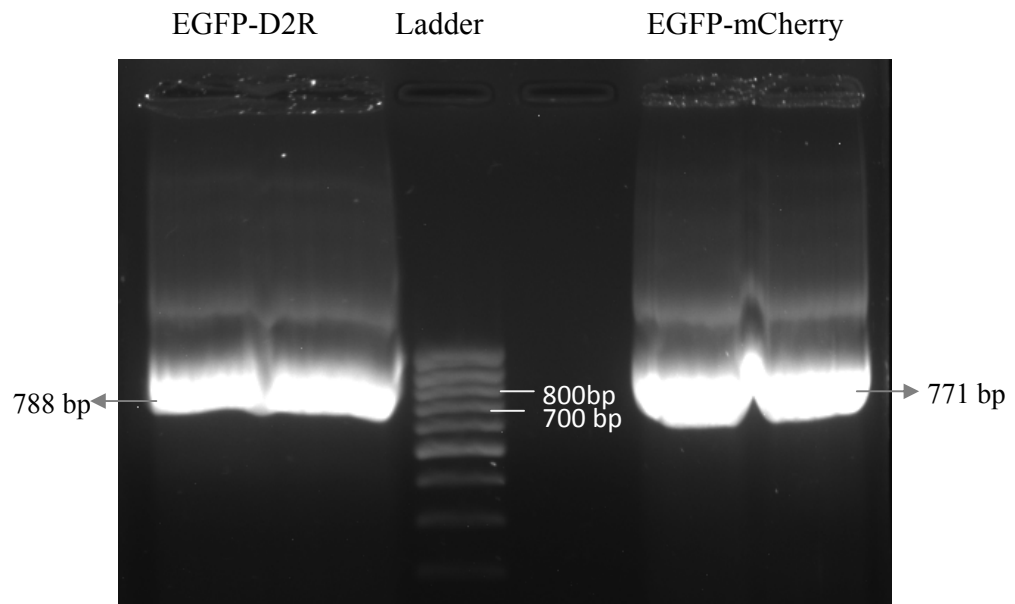
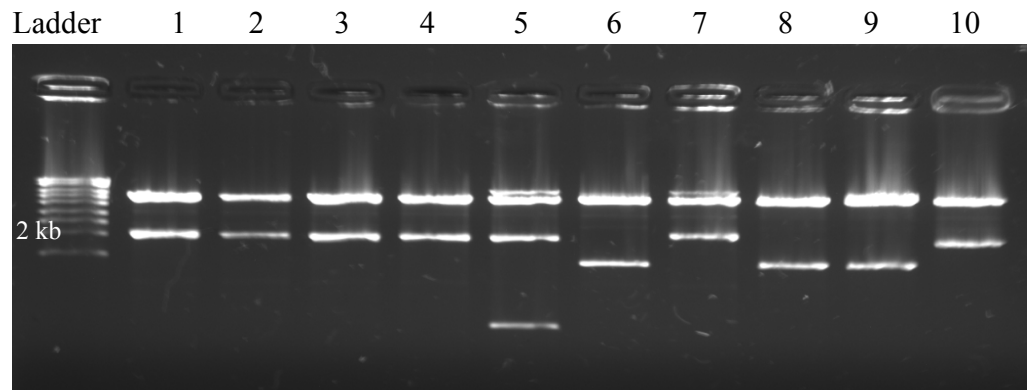


**Figure 3.17** Agarose gel electrophoresis photo of EGFP and mCherry PCR amplification with D<sub>2</sub>R flanking ends

PCR products of D2R-EGFP and D2R-mCherry were excised and extracted from the gel. Gel elution products were used for PCR integration method as primers. The template of this reaction was pcDNA 3.1 (-)D<sub>2</sub>R. After this second PCR and transformation to *E. coli*, newly synthesized plasmids were screened with double digestion and checking the insert size, which should be about 2 kb. Five colonies from D2R-EGFP plate and 3 colonies from D2R-mCherry plate were chosen.



- 1- pcDNA 3.1 (-)\_D2R-EGFP\_1
- 2- pcDNA 3.1 (-)\_D2R-EGFP\_2
- 3- pcDNA 3.1 (-)\_D2R-EGFP\_3
- 4- pcDNA 3.1 (-)\_D2R-EGFP\_4
- 5- pcDNA 3.1 (-)\_D2R-EGFP\_5
- 6- pcDNA 3.1 (-)\_D2R-mCherry\_1
- 7- pcDNA 3.1 (-)\_D2R-mCherry\_2
- 8- pcDNA 3.1 (-)\_D2R-mCherry\_3
- 9- pcDNA 3.1 (-)\_D2R (negative control)
- 10- pcDNA 3.1 (-) with a 2 kb insert (positive control)

**Figure 3.18** Agarose gel photo of *NotI-HindIII* digestion screening of candidate pcDNA 3.1 (-)\_D2R-EGFP/mCherry vectors

According to Fig. 3.18, EGFP constructs #1, #2, #3, #4 and mCherry construct #2 have the correct sizes. These constructs were transfected to N2a cell line and observed with laser scanning confocal microscope. pcDNA 3.1 (-)\_D2R-mCherry #2 could give red fluorescence (see Fig. 3.19) as it was expected to; however, none of the four D2R-EGFP constructs had fluorescent ability, which may have been due to frame shifts and/or missense mutations done by DNA polymerase during the long second PCR reaction.

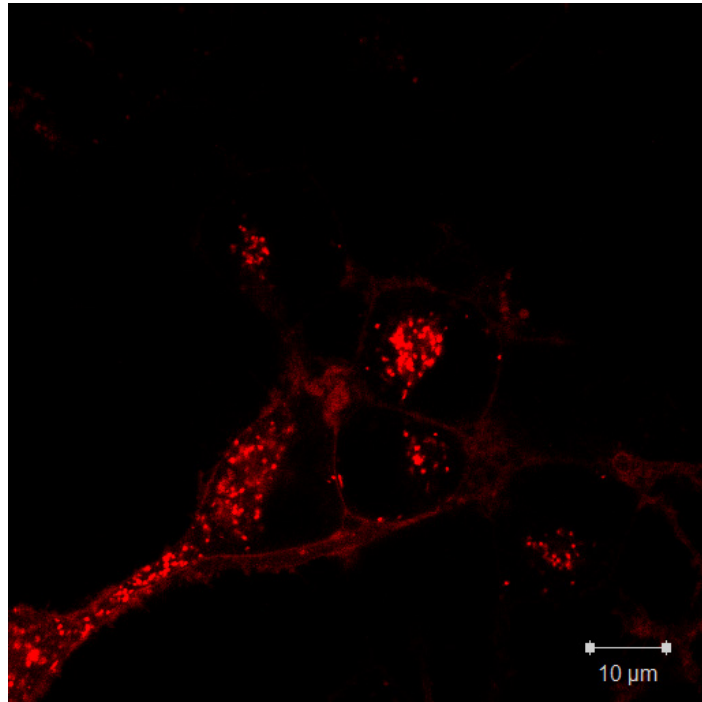


**Figure 3.19** N2a cells transfected with pcDNA 3.1 (-)\_D<sub>2</sub>R+mCherry vector, excited at 543 nm

After seeing the fluorescent signal as in Fig. 3.4.3, the construct was sent to sequencing and correct D2R-mCherry sequence was verified (see Fig. 3.20).

ATGGATCCACTGAATCTGTCCCTGGTATGATGATGATCTGGAGAGGCAGAACTGGAGCC  
 GGCCCTTCAACGGGTCAGACGGGAAGGCGGACAGACCCCACTACAACACTATGCCAC  
 ACTGCTCACCTGCTCATCGCTGTCATCGTCTTCGGCAACGTGCTGGTGTGCATGGCT  
 GTGTCCCGCGAGAAGGCGCTGCAGACCACCACCAACTACCTGATCGTCAGCCTCGCAG  
 TGGCCGACCTCCTCGTCGCCACACTGGTCATGCCCTGGGTTGTCTACCTGGAGGTGGT  
 AGGTGAGTGGAAATTCAGCAGGATTCACTGTGACATCTTCGTCACTCTGGACGTCATG  
 ATGTGCACGGCGAGCATCCTGAACTTGTGTGCCATCAGCATCGACAGGTACACAGCTG  
 TGGCCATGCCCATGCTGTACAATACGCGCTACAGCTCCAAGCGCCGGGTACCCTCAT  
 GATCTCCATCGTCTGGGTCCCTGTCTTACCATCTCCTGCCCACTCCTCTTCGGACTC  
 AATAACGCAGACCAGAACGAGTGCATCATTGCCAACC CGCCTTCGTGGTCTACTCCT  
 CCATCGTCTCCTTCTACGTGCCCTTCATTGTCACCCTGCTGGTCTACATCAAGATCTA  
 CATTGTCTCCTCCGCGAGACGCCGCAAGCGAGTCAACACCAAACGCAGCAGCCGAGCTTC  
 AGGGCCACCTGAGGGCTCCACTAAAGGGCAACTGTACTCACCCCGAGGACATGAAAC  
 TCTGCACCCTTATCATGAAGTCTAATGGGAGTTTCCAGTGAACAGGCGGAGAGTGGGA  
 GGCTGCCCGGCGAGCCCAGGAGCTGGAGATGGAGATGCTCTCCAGCACCAGCCCACCC  
 GAGAGGACCCGGTACAGCCCCATCCACCCAGCCACCACCAGCTGACTCTCCCCGACC  
 CGTCCCACCATGGTCTCCACAGCACTCCCGACAGCCCCGCCAAACCAGAGAAGAATGG  
 GCATGCCAAAGACCACCCCAAGATTGCCAAGATCTTTGAGATCCAGACCATGCCCAAT  
 GGCAAACCCGGACCTCCCTCAAGACCATGAGCCGTAGGAAGCTCTCCAGCAGAAGG  
 AGAAGAAAGCCACTCAGATGCTCGCCATTGTTCTCGGCGTGTTCATCATCTGCTGGCT  
 GCCCTTCTTCATCACACACATCCTGAACATACACTGTGACTGCAACATCCCGCCTGTC  
 CTGTACAGCGCTTCACGTGGCTGGGCTATGTCAACAGCGCCGTGAACCCCATCATCT  
 ACACCACCTTCAACATTGAGTTCCGCAAGGCCTTCTGAAGATCCTCCACTGCTAGAT  
 GGTGAGCAAGGGCGAGGAGGATAACATGGCCATCATCAAGGAGTTCATGCGCTTCAAGGTGCAC  
 ATGGAGGGCTCCGTGAACGGCCACGAGTTCGAGATCGAGGGCGAGGGCGAGGGCCGCCCTACG  
 AGGGCACCCAGACCCCAAGCTGAAGGTGACCAAGGGTGGCCCCCTGCCCTTCGCCTGGGACAT  
 CCTGTCCCCTCAGTTCATGTACGGCTCCAAGGCCTACGTGAAGCACCCCGCGACATCCCCGAC  
 TACTTGAAGCTGTCTTCCCCGAGGGCTTCAAGTGGGAGCGCGTGATGAACTTCGAGGACGGCG  
 GCGTGGTGACCGTGACCCAGGACTCCTCCCTGCAGGACGGCGAGTTCATCTACAAGGTGAAGCT  
 GCGCGGCACCAACTTCCCCTCCGACGGCCCCGTAATGCAGAAGAAGACCATGGGCTGGGAGGCC  
 TCCTCCGAGCGGATGTACCCCGAGGACGGCGCCCTGAAGGGCGAGATCAAGCAGAGGCTGAAGC  
 TGAAGGACGGCGGCCACTACGACGCTGAGGTCAAGACCACCTACAAGGCCAAGAAGCCCGTGCA  
 GCTGCCCGGCGCCTACAACGTCAACATCAAGTTGGACATCACCTCCCACAACGAGGACTACACC  
 ATCGTGGAACAGTACGAACGCGCCGAGGGCCGCCACTCCACCGGCGGCATGGACGAGCTGTACA  
 AGTAA

**Figure 3.20** Coding sequence of D<sub>2</sub>R+mCherry fusion gene. Black bases belong to D<sub>2</sub>R coding sequence (Accession Number: NM\_000795); red bases belong to mCherry cDNA (Accession Number: ACO48282)

### 3.5 Tagging A<sub>2A</sub>R and D<sub>2</sub>R with EGFP

Since the attempt of EGFP labeling of D<sub>2</sub>R was failed previously, it was included in the experiments to tag A<sub>2A</sub>R with EGFP. To amplify EGFP with D<sub>2</sub>R and A<sub>2A</sub>R flanking ends as described before, the primers shown in Appendix G were used. After PCR, products were run on agarose gel for the next gel extraction step. Agarose gel photo of these PCR products is seen below on Fig. 3.21.

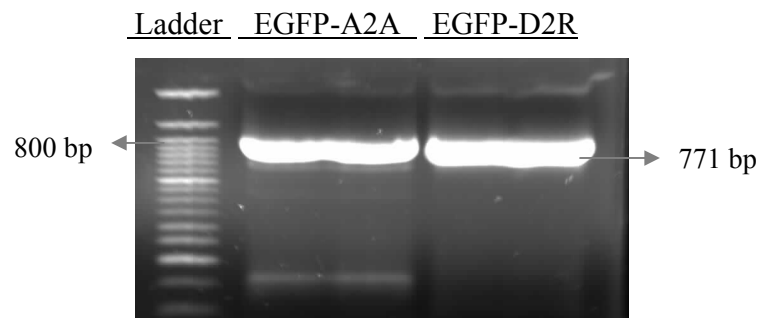
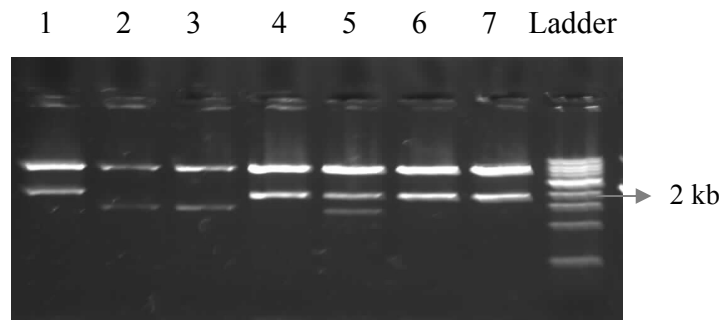


**Figure 3.21** Agarose gel electrophoresis photo of EGFP PCR amplification with A<sub>2A</sub>R and D<sub>2</sub>R flanking ends

These PCR products were excised and extracted from the gel and used in the second PCR, which is for PCR integration method. In this reaction, templates were pcDNA 3.1 (-)\_A2AR and pcDNA 3.1 (-)\_D2R vectors. Like the previous cases, products of this PCR were also transformed to *E. coli* and the plasmids of selected colonies were isolated. Plasmids were checked for the expected size (~2

kb) by double digesting them with *NotI* and *HindIII*. Results of this digestion can be seen on agarose gel photo on Fig. 3.22.



- 1- pcDNA 3.1 (-)\_D2R+EGFP#1'
- 2- pcDNA 3.1 (-)\_D2R+EGFP#2'
- 3- pcDNA 3.1 (-)\_D2R+EGFP#3'
- 4- pcDNA 3.1 (-)\_A2AR+EGFP#1
- 5- pcDNA 3.1 (-)\_A2AR+EGFP#2
- 6- pcDNA 3.1 (-)\_A2AR+EGFP #3
- 7- pcDNA 3.1 (-)\_A2AR+EGFP #4

**Figure 3.22** Agarose gel photo of *NotI-HindIII* digestion screening of candidate pcDNA 3.1 (-)\_D<sub>2</sub>R-EGFP & pcDNA 3.1 (-)\_A<sub>2</sub>A R-EGFP vectors

pcDNA 3.1 (-)\_D<sub>2</sub>R-EGFP#1' and pcDNA 3.1 (-) #1, #3 and #4 constructs had the expected size of the insert, so these four were transfected to N2a cells to test their fluorescent ability. All of them gave fluorescence; therefore, pcDNA 3.1 (-)\_D<sub>2</sub>R-EGFP #1' and pcDNA 3.1 (-)\_A<sub>2</sub>A R-EGFP #1 (see Fig.3.23 for fluorescent images) were chosen for FRET experiments.

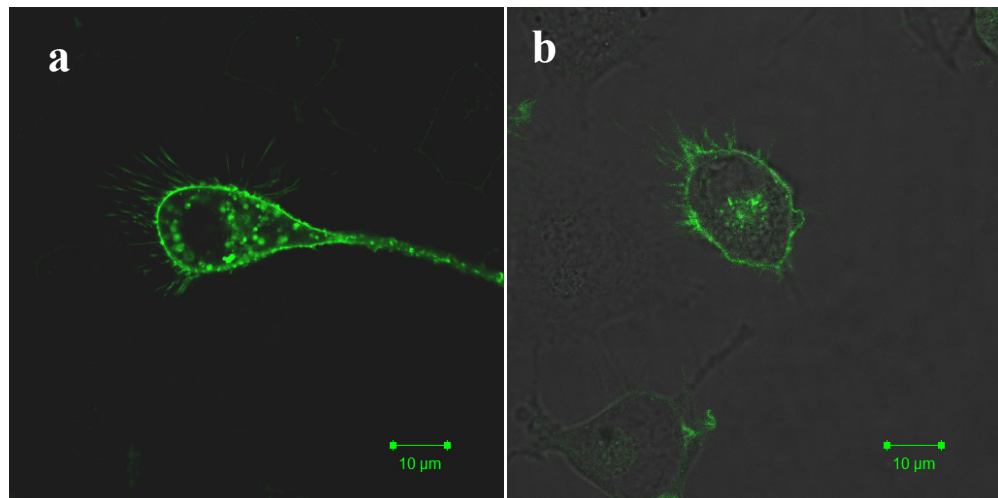


**Figure 3.23** N2a cells transfected with **a)** pcDNA 3.1 (-)\_A2AR+EGFP #1 and **b)** pcDNA 3.1 (-)\_D2R+EGFP #1' vectors, excited at 458 nm

The sequences of A2AR+EGFP and D2R+EGFP fusion constructs are shown on Fig. 3.24 and Fig 3.25, respectively.

ATGCCCATCATGGGCTCCTCGGTGTACATCACGGTGGAGCTGGCCATTGCTGTGCTGGCCATCC  
 TGGGCAATGTGCTGGTGTGCTGGGCCGTGTGGCTCAACAGCAACCTGCAGAACGTCACCAACT  
 ACTTTGTGGTGTCACTGGCGGCGGCCGACATCGCAGTGGGTGTGCTCGCCATCCCCTTTGCCAT  
 CACCATCAGCACCGGTTCTGCGCTGCCTGCCACGGCTGCCTCTTCATTGCTGCTTCGTCTG  
 GTCTCACGCAGAGCTCCATCTTCAGTCTCCTGGCCATCGCCATTGACCGCTACATTGCCATCC  
 GCATCCCCTCCGGTACAATGGCTTGGTGACCGGCACGAGGGCTAAGGGCATCATTGCCATCTG  
 CTGGGTGCTGTGCTTTGCCATCGGCCTGACTCCCATGCTAGGTTGGAACAACCTGCGGTGAGCCA  
 AAGGAGGGCAAGAACCACTCCCAGGGCTGCGGGGAGGGCCAAGTGGCCTGTCTCTTTGAGGATG  
 TGGTCCCCATGAACTACATGGTGTACTTCAACTTCTTTGCCTGTGTGCTGGTGGCCCTGTGCT  
 CATGCTGGGTGTCTATTTGCGGATCTTCTGGCGGCGCGACGACAGCTGAAGCAGATGGAGAGC  
 CAGCTCTGCCGGGGAGCGGGCACGGTCCACACTGCAGAAGGAGGTCCATGCTGCCAAGTCAC  
 TGGCCATCATTGTGGGGCTCTTTGCCCTCTGCTGGCTCATGTACATCAACATCATCAACTGCTTCC  
 TTCTTCTGCCCCGACTGCAGCCACGCCCCTCTCTGGCTCATGTACATCAACATCAACTGCTTCC  
 CACACCAATTCGGTTGTGAATCCCTTCATCTACGCCTACCGTATCCGCGAGTTCCGCCAGACCT  
 TCCGCAAGATCATTTCGAGCCACGTCTGAGGCAGCAAGAACCCTTCAAGGCAGCTGGCACCAG  
 TGCCCGGGTCTTGGCAGCTCATGGCAGTGACGGAGAGCAGGTGAGCTCCGTCTCAACGGCCAC  
 CCGCCAGGAGTGTGGGCCAACGGCAGTGTCTCCACCCTGAGCGGAGGGCCAATGGCTACGCCC  
 TGGGGCTGGTGTGAGTGGAGGGAGTGCCCAAGAGTCCCAGGGGAACACGGGCCTCCAGACGTGGA  
 GCTCCTTAGCCATGAGCTCAAGGGAGTGTGCCAGAGCCCCCTGGCCTAGATGACCCCCCTGGCC  
 CAGGATGGAGCAGGAGTGTCCATGGTGAGCAAGGGCGAGGAGCTGTTACCCGGGGTGGTGCCCA  
 TCCTGGTTCGAGCTGGACGGCGACGTAACCGGCCACAAGTTTCAGCGTGTCCGGCGAGGGCGAGGG  
 CGATGCCACCTACGGCAAGCTGACCCTGAAGTTTCATCTGCACCACCGGCAAGCTGCCCGTGCCC  
 TGGCCACCCTCGTGACCACCCTGACCTACGGCGTGCAGTGTTCAGCCGCTACCCCGACCACA  
 TGAAGCAGCAGACTTCTTCAAGTCCGCCATGCCCGAAGGCTACGTCCAGGAGCGCACCATCTT  
 CTCAAGGACGACGGCAACTACAAGACCCGCGCCGAGGTGAAGTTTCGAGGGGCGACACCCTGGTG  
 AACCGCATCGAGCTGAAGGGCATCGACTTCAAGGAGGACGGCAACATCCTGGGGCACAAGCTGG  
 AGTACAACACTACAACAGCCACAACGTCTATATCATGGCCGACAAGCAGAAGAACGGCATCAAGGT  
 GAACTTCAAGATCCGCCACAACATCGAGGACGGCAGCGTGCAGCTCGCCGACCACTACCAGCAG  
 AACACCCCATCGGGACGGCCCCGTGCTGCTGCCCGACAACCCTACCTGAGCACCAGTCCA  
 AGCTTAGCAAAGACCCCAACGAGAAGCGCGATCACATGGTCTGCTGGAGTTCGTGACCGCCG  
 CGGATCACTCTCGGCATGGACGAGCTGTACAAGTAA

**Figure 3.24** Coding sequence of A<sub>2A</sub>R+EGFP fusion gene. Black bases belong to A<sub>2A</sub>R coding sequence (Accession Number: NM\_000675); green bases belong to EGFP cDNA (Accession Number: AAB02574)

ATGGATCCACTGAATCTGTCTGGTATGATGATGATCTGGAGAGGCAGAACTGGAGCCGGCCCT  
 TCAACGGGTCAGACGGGAAGGCGGACAGACCCCACTACAACACTATGCCACACTGCTCACCCCT  
 GCTCATCGTGTGCATCGTCTTCGGCAACGTGCTGGTGTGCATGGCTGTGTCCCGCGAGAAGGCG  
 CTGCAGACCACCACCAACTACCTGATCGTCAGCCTCGCAGTGGCCGACCTCCTCGTCGCCACAC  
 TGGTCATGCCCTGGGTTGTCTACCTGGAGGTGGTAGGTGAGTGGAAATTCAGCAGGATCACTG  
 TGACATCTTCGTCACTCTGGACGTGATGATGTGCACGGCGAGCATCCTGAACTTGTGTGCCATC  
 AGCATCGACAGGTACACAGCTGTGGCCATGCCCATGCTGTACAATACGCGCTACAGCTCCAAGC  
 GCCGGGTCACCGTCATGATCTCCATCGTCTGGGTCCTGTCCCTCACCATCTCCTGCCCACTCCT  
 CTTCGGACTCAATAACGCAGACCAGAACGAGTGCATCATTGCCAACCCGGCCCTTCGTGGTCTAC  
 TCTCCATCGTCTCCTTCTACGTGCCCTTCATTGTCAACCCTGCTGGTCTACATCAAGATCTACA  
 TTGTCTCCGCAGACGCCGCAAGCGAGTCAACACCAAACGCAGCAGCCGAGCTTTCAGGGCCCA  
 CCTGAGGGCTCCACTAAAGGGCAACTGTACTCACCCCGAGGACATGAAACTCTGCACCGTTATC  
 ATGAAGTCTAATGGGAGTTTCCAGTGAACAGGCGGAGGTGGAGGCTGCCCGGCGACCCCAAGG  
 AGCTGGAGATGGAGATGCTCTCCAGCACCCAGCCACCCGAGAGGACCCGGTACAGCCCCATCCC  
 ACCCAGCCACCACCAGCTGACTCTCCCCGACCCGTCACCACCATGGTCTCCACAGCACTCCCGAC  
 AGCCCCGCCAAACCAGAGAAGAATGGGCATGCCAAAGACCACCCCAAGATTGCCAAGATCTTTG  
 AGATCCAGACCATGCCCAATGGCAAACCCGGACCTCCCTCAAGACCATGAGCCGTAGGAAGCT  
 CTCCAGCAGAAGGAGAAGAAAGCCACTCAGATGCTCGCCATTGTTCTCGGCGTGTTCATCATC  
 TGCTGGCTGCCCTTCTTCATCACACACATCCTGAACATACACTGTGACTGCAACATCCCGCCTG  
 TCTGTACAGCGCCTTACGTGGCTGGGCTATGTCAACAGCGCCGTGAACCCCATCATCTACAC  
 CACCTTCAACATTGAGTTCCGCAAGGCCTTCTGAAGATCCTCCACTGCATGGTGAGCAAGGGC  
 GAGGAGCTGTTACCCGGGGTGGTGGCCATCCTGGTTCGAGCTGGACGGCGACGTAAACGGCCACA  
 AGTTCAGCGTGTCCGGCGAGGGCGAGGGCGATGCCACCTACGGCAAGCTGACCCCTGAAGTTCAT  
 CTGCAACCCGGCAAGCTGCCCGTCCCTGGCCACCCCTCGTGACCACCCCTGACCTACGGCGTG  
 CAGTGCTTCAGCCGCTACCCCGACCACATGAAGCAGCACGACTTCTTCAAGTCCGCCATGCCCG  
 AAGGCTACGTCCAGGAGCGACCATCTTCTTCAAGGACGACGGCAACTACAAGACCCGCGCCGA  
 GGTGAAGTTCGAGGGCGACACCCTGGTGAACCGCATCGAGCTGAAGGGCATCGACTTCAAGGAG  
 GACGGCAACATCCTGGGGCACAAGCTGGAGTACAACACTACAACAGCCACAACGTCTATATCATGG  
 CCGACAAGCAGAAGAACGGCATCAAGGTGAACTTCAAGATCCGCCACAACATCGAGGACGGCAG  
 CGTGCAGCTCGCCGACCACTACCAGCAGAACACCCCATCGGCGACGGCCCCGTGCTGCTGCCC  
 GACAACCACTACCTGAGCACCCAGTCCAAGCTTAGCAAAGACCCCAACGAGAGCGCGATCACA  
 TGGTCTGCTGGAGTTTCGTGACCGCCGCGGGATCACTCTCGGCATGGACGAGCTGTACAAGTA  
 A

**Figure 3.25** Coding sequence of D<sub>2</sub>R+EGFP fusion gene. Black bases belong to D<sub>2</sub>R coding sequence (Accession Number: NM\_000795); green bases belong to EGFP cDNA sequence (Accession Number: AAB02574)

### **3.6 Optimization of Fluorescence Resonance Energy Transfer in N2a Cells Double Transfected with A<sub>2A</sub>R-EGFP & D<sub>2</sub>R-mCherry**

500 ng of pcDNA 3.1 (-)\_A<sub>2A</sub>R-EGFP and 500 ng of pcDNA 3.1 (-)\_D<sub>2</sub>R-mCherry plasmids were transfected to N2a cells using Lipofectamine<sup>TM</sup> LTX and Plus<sup>TM</sup> reagents. The cells were observed 40-48 hours after transfection. In FRET setup, two control groups were prepared as well. One group was transfected only with A<sub>2A</sub>R-EGFP; the other group was with D<sub>2</sub>R-mCherry. Transfected cells were observed with the multi-track configurations below (see Fig. 3.26, Fig. 3.27 & Fig. 3.28), accordingly.

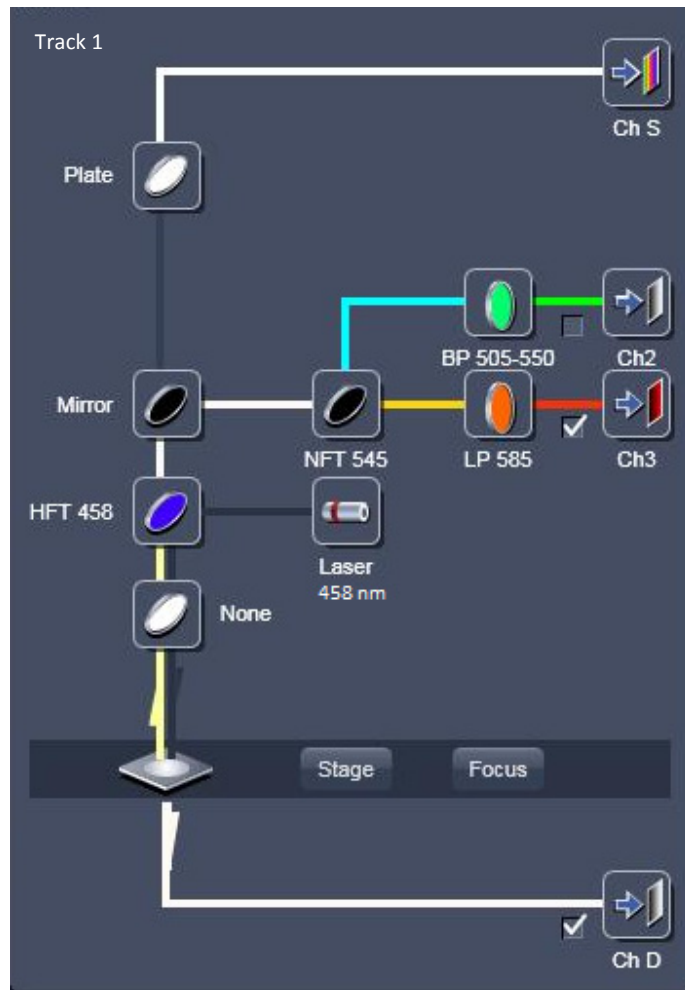


**Figure 3.26** Track 1 configuration in laser scanning confocal microscope to detect FRET in channel 3 after exciting the cell at 458 nm

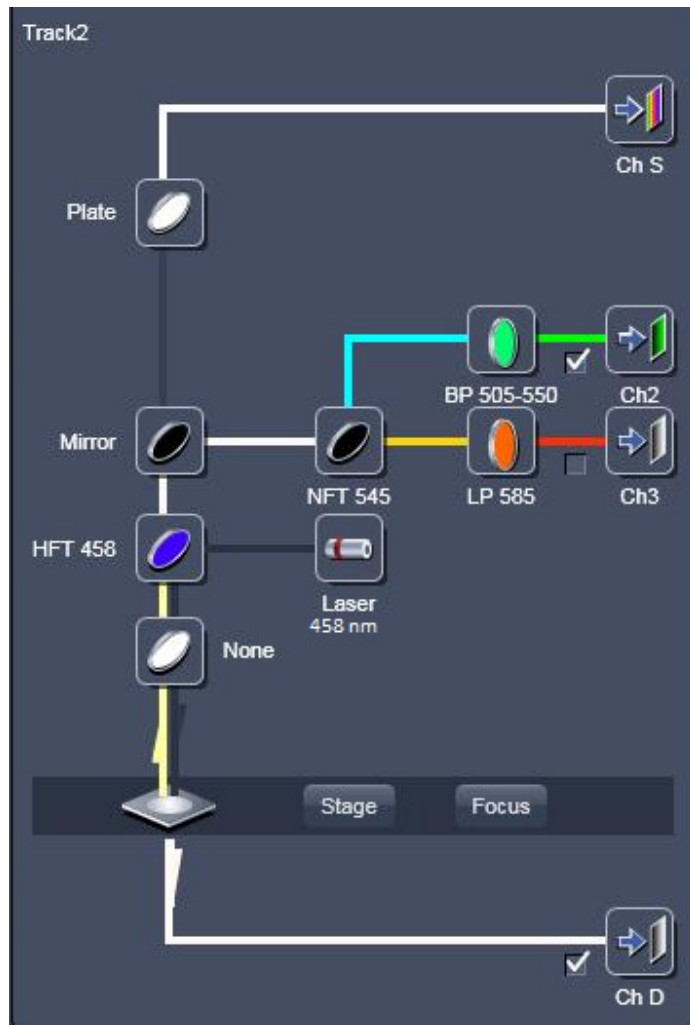


**Figure 3.27** Track 2 configuration in laser scanning confocal microscope to detect donor bleed-through in channel 2 after exciting the cell at 458 nm

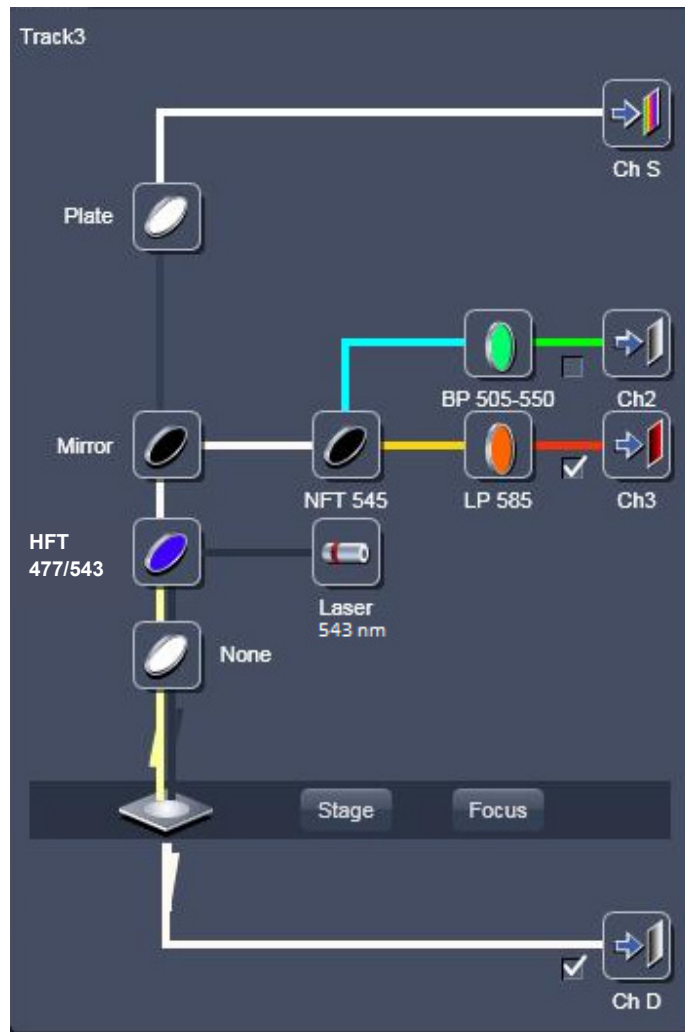


**Figure 3.28** Track 3 configuration in laser scanning confocal microscope to detect acceptor bleed in channel 3 after exciting the cell at 543 nm

Double transfected live N2a cells were observed with all of the three tracks. Track 1 image (Fig. 3.31.a) was used for normalized FRET (NFRET) calculation. Track 2 image (Fig. 3.31.b) was used to calculate and normalize donor bleed-through, in other words, how much of the green signal leaks through the red emission range. On the other hand, track 3 image (Fig. 3.31.c) was used for acceptor bleed-through, in other words, to calculate how much of channel 3 signal came from the leakage of red fluorescence possibly excited by 458 nm. Of course, it is not possible to determine the bleed-through using double transfected cells. To understand how much leakage comes from green or red fluorescent protein, they were single transfected and observed as well. As donor bleed-through control, D2R-EGFP transfected cells were observed with track 1 and 2 (Fig. 3.30); whereas, acceptor bleed through control was observed with track 1 and 3 (Fig. 3.29). These controls were stored to Pix-FRET plug-in of Image J to normalize bleed-through. For FRET computation, three images of double transfected cells taken with three of the tracks were opened in Pix-FRET and NFRET values were calculated with  $FRET/\sqrt{Donor*Acceptor}$  formula.

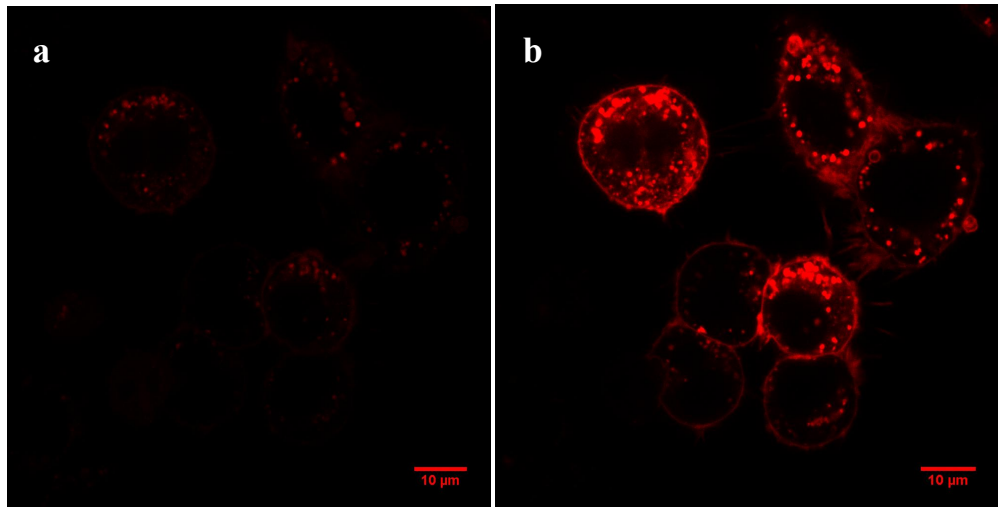


**Figure 3.29** N2a cells transfected with A<sub>2A</sub>R-mCherry observed with **a)** track 1 and **b)** track 3 as acceptor bleed-through controls

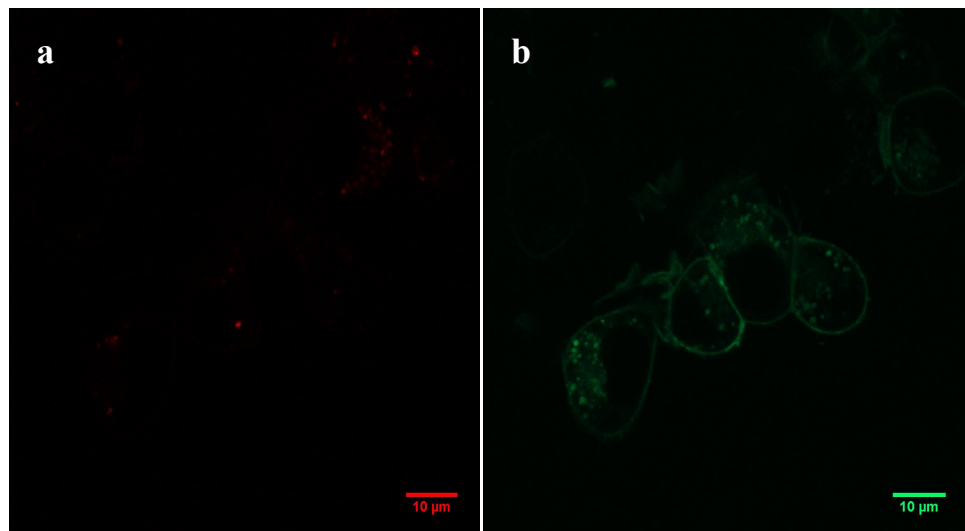


**Figure 3.30** N2a cells transfected with D<sub>2</sub>R-EGFP observed with **a)** track 1 and **b)** track 2 as acceptor bleed-through controls

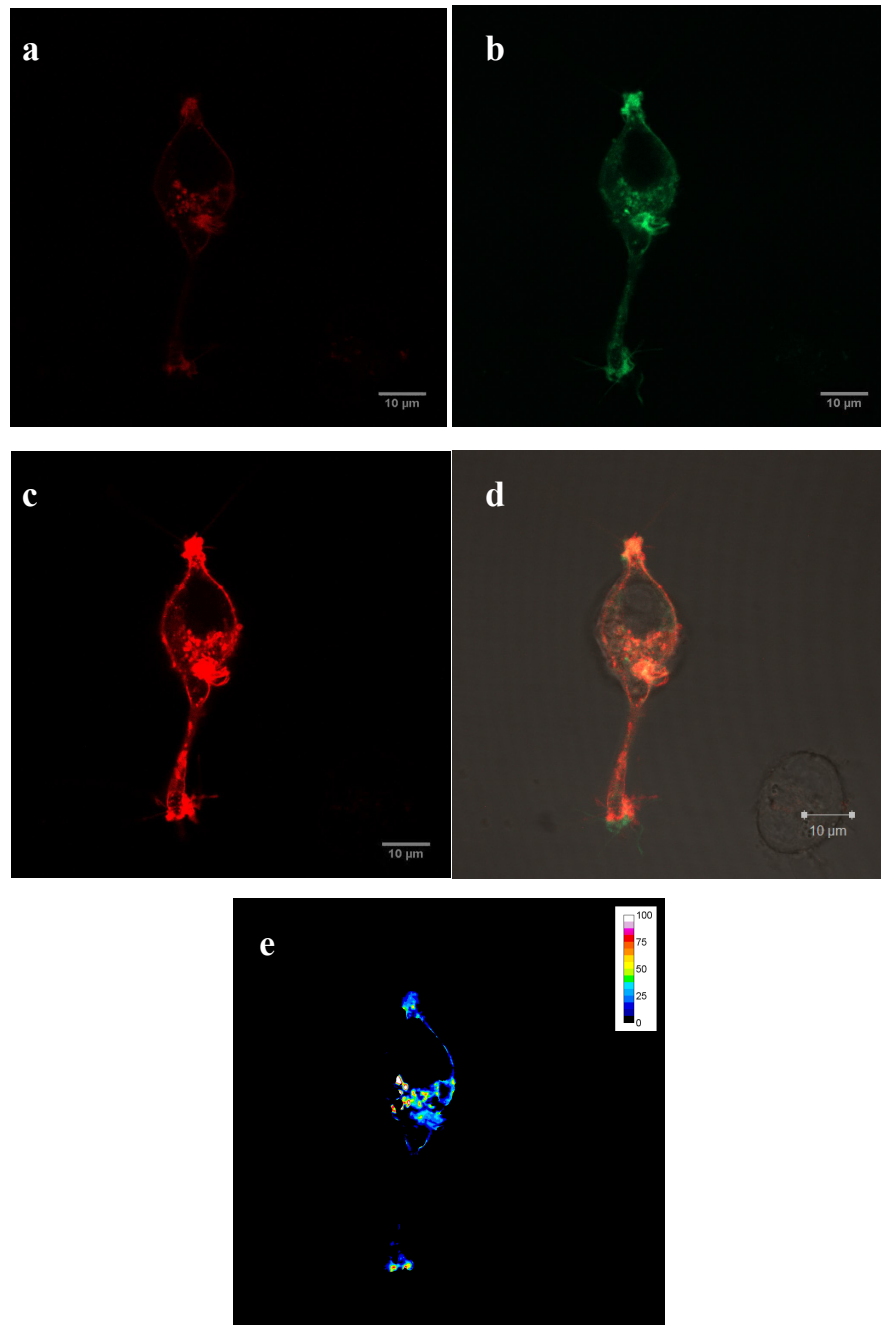


**Figure 3.31** N2a cells transfected with D<sub>2</sub>R-EGFP and A2AR-mCherry constructs observed with **a)** track 1 and **b)** track 2 **c)** track 3 and **d)** overlay of all stacks and channel D. Image **(e)** shows the pixels where NFRET occurs on the cell

Fig. 3.31.e shows where on the cell FRET occurs. As it can be seen, FRET signal is detected on the membrane as a thin line around the cell, though it is relatively low compared to the internal vesicular structures. Higher FRET signals are seen on the intracellular compartments, which may possibly be around ER and Golgi apparatus. These are the sites where vesicles loaded with membrane proteins are concentrated during their synthesis and trafficking. Yet, it is necessary to analyze more cells to make a statistically significant conclusion. By looking at the intracellular FRET signals, it may be hypothesized that adenosine A<sub>2A</sub> and dopamine D<sub>2</sub> receptors may dimerize early in ER and/or Golgi. This hypothesis should, of course, be tested using organelle markers and other experimental setups. It is also required to design agonist/antagonist introduction experiments to see how dimerization of dopamine D<sub>2</sub> and adenosine A<sub>2A</sub> receptors on the membrane would be affected.

## CHAPTER IV

### CONCLUSION

The aim of this thesis was to design and construct fluorescently tagged adenosine A<sub>2A</sub> and dopamine D<sub>2</sub> receptors; express them in live N2a mouse neuroblastoma cell line and optimize the FRET method to detect the interaction between these two receptors.

At the end of this study, both receptors could successfully be labeled from their C-termini with both EGFP and mCherry fluorescent proteins to observe FRET in reciprocal setups, either A<sub>2A</sub>R-mCherry & D<sub>2</sub>R-EGFP or A<sub>2A</sub>R-EGFP & D<sub>2</sub>R-mCherry. The purpose of designing reciprocal FRET pairs is to show the specificity of the setup, in other words, FRET is independent of choice the receptor-fluorescent protein label. Though only A<sub>2A</sub>R-mCherry & D<sub>2</sub>R-EGFP pair was analyzed in this thesis, other pair is remained to be analyzed in further studies.

Functionality and sequence of the fusion receptor constructs were confirmed. The configurations of multi-track setup were determined by repeated imaging experiments. The final and optimized FRET multi-track configuration in laser scanning microscope was presented with this thesis study.

As a double confirmation to FRET, bimolecular fluorescence complementation assay (BiFC) assay to detect the interaction between D<sub>2</sub>R and A<sub>2A</sub>R was planned

to be done. First trial experiments was completed; however, the results of these trials are not presented in this thesis because more trials and further imaging experiments should be done. Using PCR integration method, A<sub>2A</sub>R was labeled with the first 128 amino acid of EGFP; whereas, D<sub>2</sub>R was labeled with the last 110 amino acid of EGFP. Both of these fragments had no green fluorescence; however, they would regain their fluorescence ability upon complementation of the EGFP fragments if two receptors interact. Although the results of this project were not shown here, sequence verified constructs were designed, transfected to N2a cells and observed with laser scanning confocal microscope with success. However, no detectable signal could be observed at this position of insertion. The reasons of the failure may not be due to the lack of interaction, but due to the choice of the position of splitting EGFP or the position on the receptor where these split EGFP fragments were added. In short, BiFC method to detect A<sub>2A</sub>R-D<sub>2</sub>R interaction remains to be optimized for future studies.

The results of this project present optimized constructs and conditions to detect heterodimerization of physiologically important two G-protein coupled receptors, dopamine D<sub>2</sub> and adenosine A<sub>2A</sub> receptors. Using FRET method, possible antipsychotics, drugs targeted to neurophysiological disorders, dopamine and adenosine agonists/antagonists can be tested to observe if they have any inhibitory/stimulatory effects on dimerization; and therefore, on dopamine and adenosine signaling, which take essentially important roles in food intake, memory, learning and control of motor functions.

With this thesis study, a powerful, fluorescence based cell culture model to detect the hetero-dimerization of adenosine A<sub>2A</sub> and dopamine D<sub>2</sub> receptors has been successfully developed. This model system is readily usable for drug screening research. Drugs that affect dopamine or adenosine signaling can be introduced to this system and their effect on hetero-dimerization of these

receptors can be investigated very easily. Thus, this system is also useful to study/screen molecular mechanisms of some chemicals as potential drugs.

## REFERENCES

- Albertazzi, L., Arosio, D., Marchetti, L., Ricci, F., & Beltram, F. (2009). Quantitative FRET analysis with the EGFP-mCherry fluorescent protein pair. *Photochem Photobiol*, 85(1), 287-297.
- Angers, S., Salahpour, A., & Bouvier, M. (2002). Dimerization: an emerging concept for G protein-coupled receptor ontogeny and function. *Annu Rev Pharmacol Toxicol*, 42, 409-435.
- Angers, S., Salahpour, A., Joly, E., Hilairet, S., Chelsky, D., Dennis, M., et al. (2000). Detection of 2-adrenergic receptor dimerization in living cells using bioluminescence resonance energy transfer (BRET). *Proc Natl Acad Sci U S A*, 97(7), 3684-3689.
- Ayoub, M. A., Couturier, C., Lucas-Meunier, E., Angers, S., Fossier, P., Bouvier, M., et al. (2002). Monitoring of ligand-independent dimerization and ligand-induced conformational changes of melatonin receptors in living cells by bioluminescence resonance energy transfer. *J Biol Chem*, 277(24), 21522-21528.
- Babcock, G. J., Farzan, M., & Sodroski, J. (2003). Ligand-independent dimerization of CXCR4, a principal HIV-1 coreceptor. *J Biol Chem*, 278(5), 3378-3385.
- Baneres, J. L., & Parello, J. (2003). Structure-based analysis of GPCR function: evidence for a novel pentameric assembly between the dimeric leukotriene B4 receptor BLT1 and the G-protein. *J Mol Biol*, 329(4), 815-829.
- Bara-Jimenez, W., Sherzai, A., Dimitrova, T., Favit, A., Bibbiani, F., Gillespie, M., et al. (2003). Adenosine A(2A) receptor antagonist treatment of Parkinson's disease. *Neurology*, 61(3), 293-296.

- Benarroch, E. E. (2008). Adenosine and its receptors: multiple modulatory functions and potential therapeutic targets for neurologic disease. *Neurology*, 70(3), 231-236.
- Blum, D., Hourez, R., Galas, M. C., Popoli, P., & Schiffmann, S. N. (2003). Adenosine receptors and Huntington's disease: implications for pathogenesis and therapeutics. *Lancet Neurol*, 2(6), 366-374.
- Bouvier, M. (2001). Oligomerization of G-protein-coupled transmitter receptors. [10.1038/35067575]. *Nat Rev Neurosci*, 2(4), 274-286.
- Bulenger, S., Marullo, S., & Bouvier, M. (2005). Emerging role of homo- and heterodimerization in G-protein-coupled receptor biosynthesis and maturation. *Trends Pharmacol Sci*, 26(3), 131-137.
- Cadigan, K. M., & Liu, Y. I. (2006). Wnt signaling: complexity at the surface. *J Cell Sci*, 119(Pt 3), 395-402.
- Choi, E.-J., Xia, Z., Villacres, E. C., & Storm, D. R. (1993). The regulatory diversity of the mammalian adenylyl cyclases. *Current Opinion in Cell Biology*, 5(2), 269-273.
- Civelli, O., Bunzow, J. R., & Grandy, D. K. (1993). Molecular diversity of the dopamine receptors. *Annu Rev Pharmacol Toxicol*, 33, 281-307.
- Conlon, B. A., Ross, J. D., & Law, W. R. (2005). Advances in understanding adenosine as a plurisystem modulator in sepsis and the systemic inflammatory response syndrome (SIRS). *Front Biosci*, 10, 2548-2565.
- Cornea, A., Janovick, J. A., Maya-Nunez, G., & Conn, P. M. (2001). Gonadotropin-releasing hormone receptor microaggregation. Rate monitored by fluorescence resonance energy transfer. *J Biol Chem*, 276(3), 2153-2158.
- Crespo, P., Xu, N., Simonds, W. F., & Gutkind, J. S. (1994). Ras-dependent activation of MAP kinase pathway mediated by G-protein [beta][gamma] subunits. [10.1038/369418a0]. *Nature*, 369(6479), 418-420.
- Dal Toso, R., Sommer, B., Ewert, M., Herb, A., Pritchett, D. B., Bach, A., et al. (1989). The dopamine D2 receptor: two molecular forms generated by alternative splicing. *EMBO J*, 8(13), 4025-4034.
- Dorsam, R. T., & Gutkind, J. S. (2007). G-protein-coupled receptors and cancer. *Nat Rev Cancer*, 7(2), 79-94.

- Dunwiddie, T. V., & Masino, S. A. (2001). The role and regulation of adenosine in the central nervous system. *Annu Rev Neurosci*, *24*, 31-55.
- During, M. J., & Spencer, D. D. (1992). Adenosine: a potential mediator of seizure arrest and postictal refractoriness. *Ann Neurol*, *32*(5), 618-624.
- Feige, J. N., Sage, D., Wahli, W., Desvergne, B., & Gelman, L. (2005). PixFRET, an ImageJ plug-in for FRET calculation that can accommodate variations in spectral bleed-throughs. *Microsc Res Tech*, *68*(1), 51-58.
- Ferre, S., Ciruela, F., Canals, M., Marcellino, D., Burgueno, J., Casado, V., et al. (2004). Adenosine A2A-dopamine D2 receptor-receptor heteromers. Targets for neuro-psychiatric disorders. *Parkinsonism Relat Disord*, *10*(5), 265-271.
- Ferre, S., Fredholm, B. B., Morelli, M., Popoli, P., & Fuxe, K. (1997). Adenosine-dopamine receptor-receptor interactions as an integrative mechanism in the basal ganglia. *Trends Neurosci*, *20*(10), 482-487.
- Ferre, S., von Euler, G., Johansson, B., Fredholm, B. B., & Fuxe, K. (1991). Stimulation of high-affinity adenosine A2 receptors decreases the affinity of dopamine D2 receptors in rat striatal membranes. *Proc Natl Acad Sci U S A*, *88*(16), 7238-7241.
- Fotiadis, D., Liang, Y., Filipek, S., Saperstein, D. A., Engel, A., & Palczewski, K. (2003). Atomic-force microscopy: Rhodopsin dimers in native disc membranes. *Nature*, *421*(6919), 127-128.
- Fredholm, B. B., Chen, J. F., Masino, S. A., & Vaugeois, J. M. (2005). Actions of adenosine at its receptors in the CNS: insights from knockouts and drugs. *Annu Rev Pharmacol Toxicol*, *45*, 385-412.
- Fredriksson, R., Lagerström, M. C., Lundin, L. G., & Schiöth, H. B. (2003). The G-protein-coupled receptors in the human genome form five main families. Phylogenetic analysis, paralogon groups, and fingerprints. *Mol Pharmacol*, *63*(6), 1256-1272.
- Gingrich, J. A., & Caron, M. G. (1993). Recent advances in the molecular biology of dopamine receptors. *Annu Rev Neurosci*, *16*, 299-321.
- Hague, C., Uberti, M. A., Chen, Z., Bush, C. F., Jones, S. V., Ressler, K. J., et al. (2004). Olfactory receptor surface expression is driven by association

- with the 2-adrenergic receptor. *Proc Natl Acad Sci U S A*, 101(37), 13672-13676.
- Hague, C., Uberti, M. A., Chen, Z., Hall, R. A., & Minneman, K. P. (2004). Cell surface expression of alpha1D-adrenergic receptors is controlled by heterodimerization with alpha1B-adrenergic receptors. *J Biol Chem*, 279(15), 15541-15549.
- Hebert, T. E., Moffett, S., Morello, J. P., Loisel, T. P., Bichet, D. G., Barret, C., et al. (1996). A peptide derived from a beta2-adrenergic receptor transmembrane domain inhibits both receptor dimerization and activation. *J Biol Chem*, 271(27), 16384-16392.
- Hepler, J. R., & Gilman, A. G. (1992). G proteins. *Trends Biochem Sci*, 17(10), 383-387.
- Herrick-Davis, K., Grinde, E., & Mazurkiewicz, J. E. (2004). Biochemical and biophysical characterization of serotonin 5-HT2C receptor homodimers on the plasma membrane of living cells. *Biochemistry*, 43(44), 13963-13971.
- Hillion, J., Canals, M., Torvinen, M., Casado, V., Scott, R., Terasmaa, A., et al. (2002). Coaggregation, cointernalization, and codesensitization of adenosine A2A receptors and dopamine D2 receptors. *J Biol Chem*, 277(20), 18091-18097.
- Issafras, H., Angers, S., Bulenger, S., Blanpain, C., Parmentier, M., Labbe-Jullie, C., et al. (2002). Constitutive agonist-independent CCR5 oligomerization and antibody-mediated clustering occurring at physiological levels of receptors. *J Biol Chem*, 277(38), 34666-34673.
- Jaakola, V. P., Griffith, M. T., Hanson, M. A., Cherezov, V., Chien, E. Y., Lane, J. R., et al. (2008). The 2.6 angstrom crystal structure of a human A2A adenosine receptor bound to an antagonist. *Science*, 322(5905), 1211-1217.
- Jackson, D. M., & Westlind-Danielsson, A. (1994). Dopamine receptors: molecular biology, biochemistry and behavioural aspects. *Pharmacol Ther*, 64(2), 291-370.
- Jordan, B. A., Trapaidze, N., Gomes, I., Nivarthi, R., & Devi, L. A. (2001). Oligomerization of opioid receptors with 2-adrenergic receptors: A role in trafficking and mitogen-activated protein kinase activation. *Proc Natl Acad Sci U S A*, 98(1), 343-348.

- King, A. E., Ackley, M. A., Cass, C. E., Young, J. D., & Baldwin, S. A. (2006). Nucleoside transporters: from scavengers to novel therapeutic targets. *Trends Pharmacol Sci*, 27(8), 416-425.
- Klabunde, T., & Hessler, G. (2002). Drug design strategies for targeting G-protein-coupled receptors. *Chembiochem*, 3(10), 928-944.
- Klco, J. M., Lassere, T. B., & Baranski, T. J. (2003). C5a receptor oligomerization. I. Disulfide trapping reveals oligomers and potential contact surfaces in a G protein-coupled receptor. *J Biol Chem*, 278(37), 35345-35353.
- Kniazeff, J., Bessis, A. S., Maurel, D., Ansanay, H., Prézeau, L., & Pin, J. P. (2004). Closed state of both binding domains of homodimeric mGlu receptors is required for full activity. *Nat Struct Mol Biol*, 11(8), 706-713.
- Kobilka, B. K. (2007). G protein coupled receptor structure and activation. *Biochim Biophys Acta*, 1768(4), 794-807.
- Lambright, D. G., Sondek, J., Bohm, A., Skiba, N. P., Hamm, H. E., & Sigler, P. B. (1996). The 2.0 Å crystal structure of a heterotrimeric G protein. *Nature*, 379(6563), 311-319.
- Lawford, B. R., Young, R., Noble, E. P., Kann, B., & Ritchie, T. (2006). The D2 dopamine receptor (DRD2) gene is associated with co-morbid depression, anxiety and social dysfunction in untreated veterans with post-traumatic stress disorder. *Eur Psychiatry*, 21(3), 180-185.
- Li, H. Z., Guo, J., Gao, J., Han, L. P., Jiang, C. M., Li, H. X., et al. (2011). Role of dopamine D2 receptors in ischemia/reperfusion induced apoptosis of cultured neonatal rat cardiomyocytes. *J Biomed Sci*, 18, 18.
- Marshall, F. H., Jones, K. A., Kaupmann, K., & Bettler, B. (1999). GABAB receptors - the first 7TM heterodimers. *Trends Pharmacol Sci*, 20(10), 396-399.
- Milligan, G. (2004a). Applications of bioluminescence- and fluorescence resonance energy transfer to drug discovery at G protein-coupled receptors. *Eur J Pharm Sci*, 21(4), 397-405.
- Milligan, G. (2004b). G protein-coupled receptor dimerization: function and ligand pharmacology. *Mol Pharmacol*, 66(1), 1-7.

- Milligan, G., & Bouvier, M. (2005). Methods to monitor the quaternary structure of G protein-coupled receptors. *FEBS J*, 272(12), 2914-2925.
- Min, C., Cho, D. I., Kwon, K. J., Kim, K. S., Shin, C. Y., & Kim, K. M. (2011). Novel Regulatory Mechanism of Canonical Wnt Signaling by Dopamine D2 Receptor through Direct Interaction with  $\beta$ -catenin. *Mol Pharmacol*.
- Missale, C., Nash, S. R., Robinson, S. W., Jaber, M., & Caron, M. G. (1998). Dopamine receptors: from structure to function. *Physiol Rev*, 78(1), 189-225.
- Monnot, C., Bihoreau, C., Conchon, S., Curnow, K. M., Corvol, P., & Clauser, E. (1996). Polar residues in the transmembrane domains of the type 1 angiotensin II receptor are required for binding and coupling. Reconstitution of the binding site by co-expression of two deficient mutants. *J Biol Chem*, 271(3), 1507-1513.
- Neer, E. J. (1995). Heterotrimeric G proteins: organizers of transmembrane signals *Cell* (Vol. 80, pp. 249-257). United States.
- Olah, M. E., & Stiles, G. L. (1995). Adenosine receptor subtypes: characterization and therapeutic regulation. *Annu Rev Pharmacol Toxicol*, 35, 581-606.
- Overton, M. C., & Blumer, K. J. (2000). G-protein-coupled receptors function as oligomers in vivo. *Curr Biol*, 10(6), 341-344.
- Park, P. S., Filipek, S., Wells, J. W., & Palczewski, K. (2004). Oligomerization of G protein-coupled receptors: past, present, and future. *Biochemistry*, 43(50), 15643-15656.
- Rashid, A. J., O'Dowd, B. F., Verma, V., & George, S. R. (2007). Neuronal Gq/11-coupled dopamine receptors: an uncharted role for dopamine. *Trends Pharmacol Sci*, 28(11), 551-555.
- Ribeiro, J. A. (2005). What can adenosine neuromodulation do for neuroprotection? *Curr Drug Targets CNS Neurol Disord*, 4(4), 325-329.
- Salahpour, A., Angers, S., Mercier, J. F., Lagace, M., Marullo, S., & Bouvier, M. (2004). Homodimerization of the beta2-adrenergic receptor as a prerequisite for cell surface targeting. *J Biol Chem*, 279(32), 33390-33397.

- Sawynok, J., & Liu, X. J. (2003). Adenosine in the spinal cord and periphery: release and regulation of pain. *Prog Neurobiol*, 69(5), 313-340.
- Schapira, A. H., Bezard, E., Brotchie, J., Calon, F., Collingridge, G. L., Ferger, B., et al. (2006). Novel pharmacological targets for the treatment of Parkinson's disease *Nat Rev Drug Discov* (Vol. 5, pp. 845-854). England.
- Schwarzschild, M. A., Agnati, L., Fuxe, K., Chen, J. F., & Morelli, M. (2006). Targeting adenosine A2A receptors in Parkinson's disease. *Trends Neurosci*, 29(11), 647-654.
- Shi, Y., Liu, X., Gebremedhin, D., Falck, J. R., Harder, D. R., & Koehler, R. C. (2008). Interaction of mechanisms involving epoxyeicosatrienoic acids, adenosine receptors, and metabotropic glutamate receptors in neurovascular coupling in rat whisker barrel cortex. *J Cereb Blood Flow Metab*, 28(1), 111-125.
- Shimomura, O., Johnson, F. H., & Saiga, Y. (1962). Extraction, purification and properties of aequorin, a bioluminescent protein from the luminous hydromedusan, Aequorea. *J Cell Comp Physiol*, 59, 223-239.
- Souza, B. R., Romano-Silva, M. A., & Tropepe, V. (2011). Dopamine d2 receptor activity modulates akt signaling and alters GABAergic neuron development and motor behavior in zebrafish larvae. *J Neurosci*, 31(14), 5512-5525.
- Strader, C. D., Fong, T. M., Tota, M. R., Underwood, D., & Dixon, R. A. (1994). Structure and function of G protein-coupled receptors. *Annu Rev Biochem*, 63, 101-132.
- Strader, C. D., Sigal, I. S., & Dixon, R. A. (1989). Structural basis of beta-adrenergic receptor function. *FASEB J*, 3(7), 1825-1832.
- Takeda, S., Kadowaki, S., Haga, T., Takaesu, H., & Mitaku, S. (2002). Identification of G protein-coupled receptor genes from the human genome sequence. *FEBS Lett*, 520(1-3), 97-101.
- Terrillon, S., & Bouvier, M. (2004). Roles of G-protein-coupled receptor dimerization: From ontogeny to signalling regulation. *EMBO Rep*, 5(1), 30-34.

- Terrillon, S., Durroux, T., Mouillac, B., Breit, A., Ayoub, M. A., Taulan, M., et al. (2003). Oxytocin and vasopressin V1a and V2 receptors form constitutive homo- and heterodimers during biosynthesis. *Mol Endocrinol*, 17(4), 677-691.
- Thanos, P. K., Rivera, S. N., Weaver, K., Grandy, D. K., Rubinstein, M., Umegaki, H., et al. (2005). Dopamine D2R DNA transfer in dopamine D2 receptor-deficient mice: effects on ethanol drinking. *Life Sci*, 77(2), 130-139.
- Tsien, R. Y. (1998). The green fluorescent protein. *Annu Rev Biochem*, 67, 509-544.
- Vallone, D., Picetti, R., & Borrelli, E. (2000). Structure and function of dopamine receptors. *Neurosci Biobehav Rev*, 24(1), 125-132.
- Végh, A., Papp, J. G., Semeraro, C., Fatehi-Hasanabad, Z., & Parratt, J. R. (1998). The dopamine receptor agonist Z1046 reduces ischaemia severity in a canine model of coronary artery occlusion. *Eur J Pharmacol*, 344(2-3), 203-213.

## APPENDIX A

### METABOLIC REACTIONS

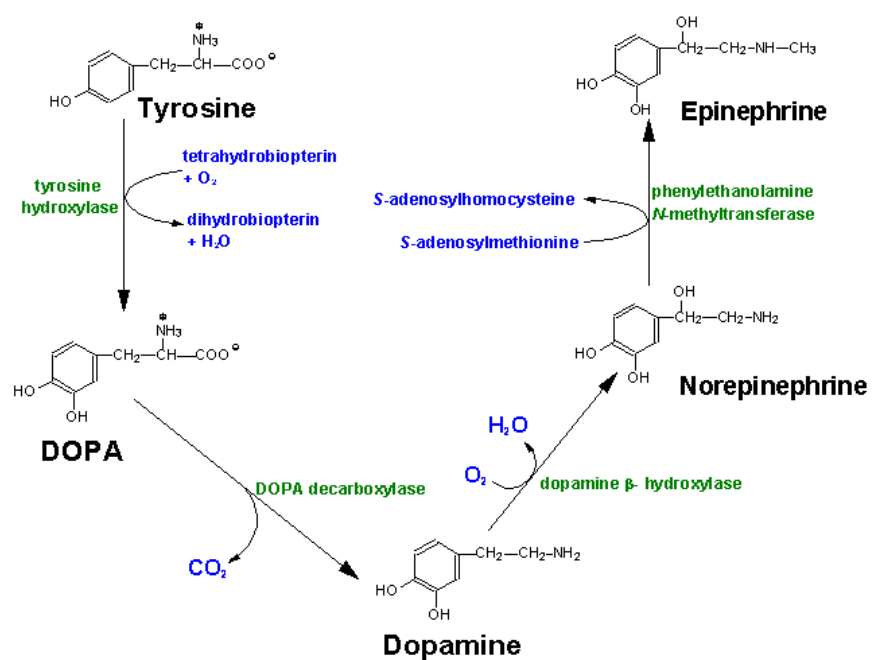


**Figure A.1** Metabolic reactions of dopamine (adapted from <http://www.bio.davidson.edu>)

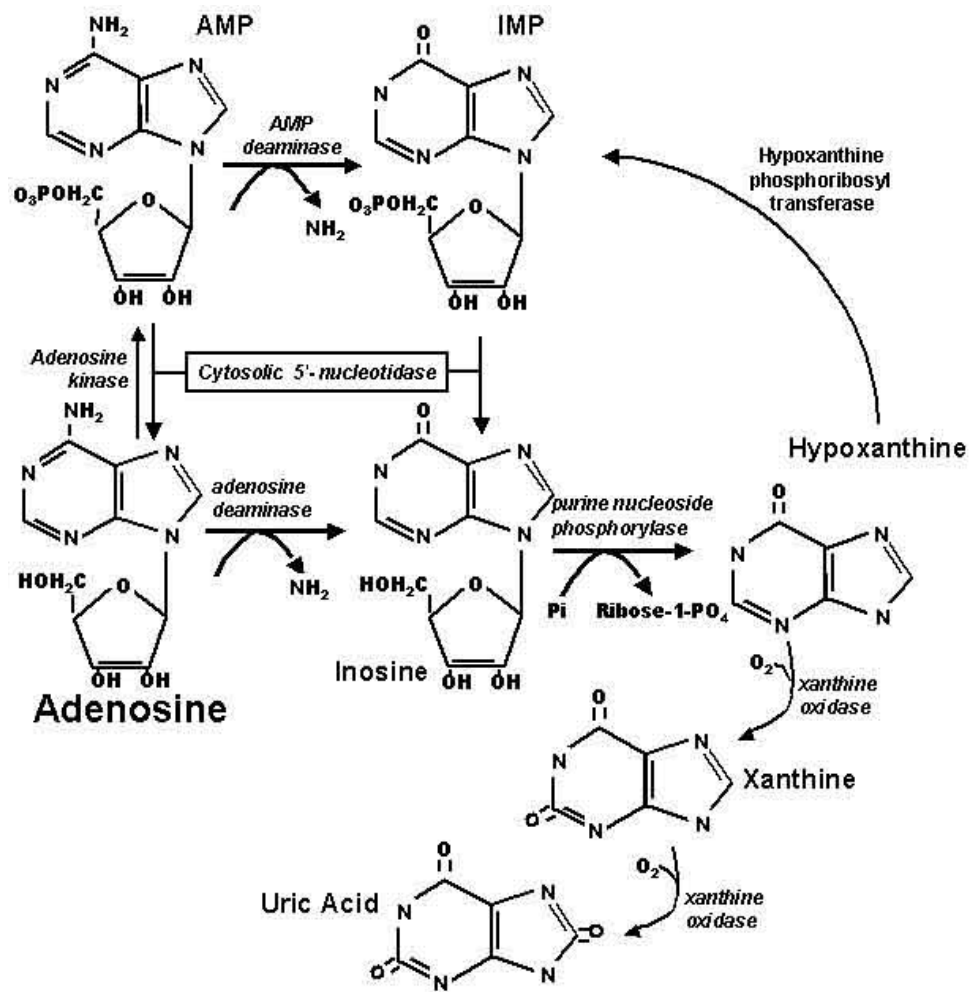
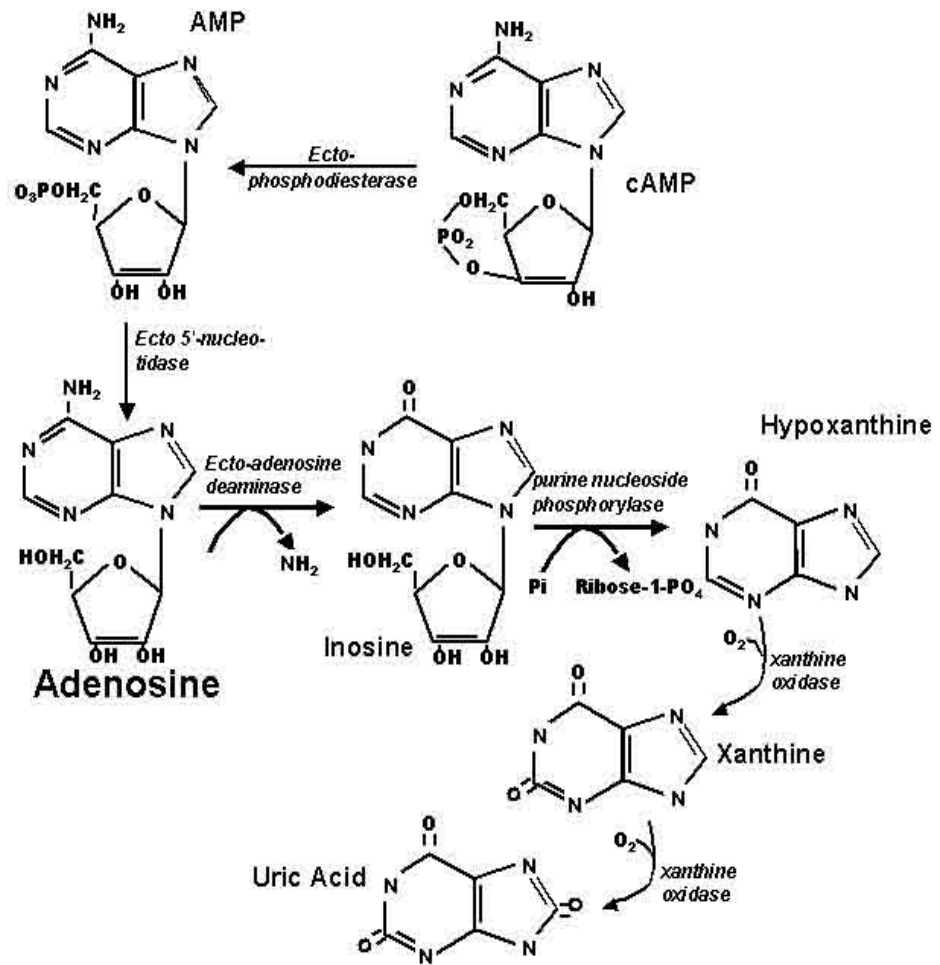
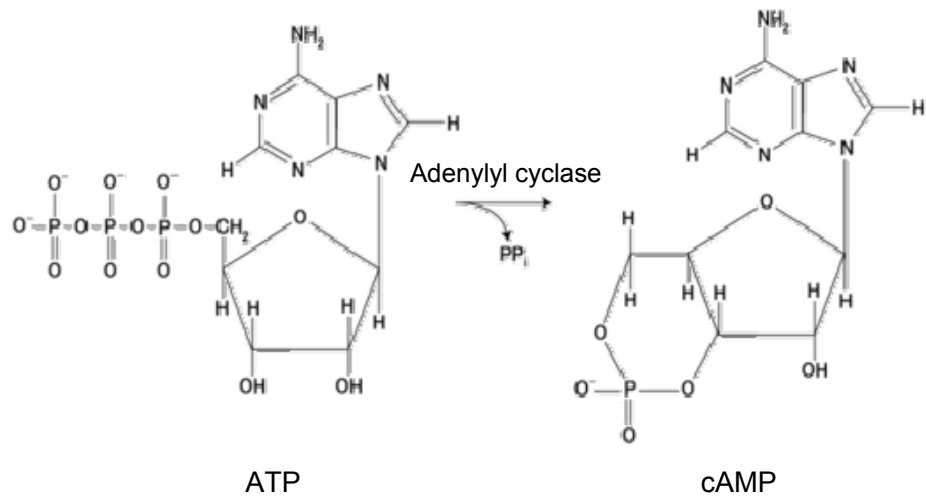


Figure A.2 Intracellular metabolism of adenosine (Conlon, et al., 2005)



**Figure A.3** Extracellular metabolism of adenosine (Conlon, et al., 2005)



**Figure A.4** Conversion of ATP to cAMP by the action of adenylyl cyclase

## APPENDIX B

### NEURO2A CELL CULTURE MEDIUM

**Table B.1 Composition of D-MEM with High Glucose**

COMPONENT	CONCENTRATION (mg/L)
<i>Amino Acids</i>	
Glycine	30
L-Arginine hydrochloride	84
L-Cysteine 2HCl	63
L-Glutamine	580
L-Histidine hydrochloride-H <sub>2</sub> O	42
L-Isoleucine	105
L-Leucine	105
L-Lysine hydrochloride	146
L-Methionine	30
L-Phenylalanine	66
L-Serine	42
L-Threonine	95
L-Tryptophan	16
L-Tyrosine	72
L-Valine	94
<i>Vitamins</i>	
Choline chloride	4

**Table B.1 cont'd Composition of D-MEM with High Glucose**

D-Calcium pantothenate	4
Folic acid	4
Niacinamide	4
Pyridoxine hydrochloride	4
Riboflavin	0.4
Thiamine hydrochloride	4
i-Inositol	7.2
<b><i>Inorganic Salts</i></b>	
Calcium chloride	264
Ferric nitrate	0.1
Magnesium sulfate	200
Potassium chloride	400
Sodium bicarbonate	3700
Sodium chloride	6400
Sodium phosphate monobasic	141
<b><i>Other components</i></b>	
D-Glucose (Dextrose)	4500
Phenol Red	15
Sodium pyruvate	110

## **APPENDIX C**

### **BACTERIAL CULTURE MEDIA PREPARATION**

#### **Luria- Bertani (LB) Medium**

10 g/L tryptone

5 g /L yeast extract

5 g/L NaCl

15 g/L agar is added to LB for solid agar medium preparation.

## APPENDIX D

### BUFFERS & SOLUTIONS

#### **1X NEBuffer 1:**

10 mM Bis-Tris-Propane-HCl

10 mM MgCl<sub>2</sub>

1 mM Dithiothreitol

pH 7.0 at 25°C

#### **1X NEBuffer 2:**

10 mM Tris-HCl

50 mM NaCl

10 mM MgCl<sub>2</sub>

1 mM Dithiothreitol

pH 7.9 at 25°C

#### **1X NEBuffer 3:**

50 mM Tris-HCl

100 mM NaCl

10 mM MgCl<sub>2</sub>

1 mM Dithiothreitol

pH 7.9 at 25°C

**1X NEBuffer 4:**

20 mM Tris-acetate  
50 mM potassium acetate  
10 mM Magnesium Acetate  
1 mM Dithiothreitol  
pH 7.9 at 25°C

**1X T4 DNA Ligase Reaction Buffer:**

50 mM Tris-HCl  
10 mM MgCl<sub>2</sub>  
1 mM ATP  
10 mM Dithiothreitol  
pH 7.5 at 25°C

**10X TBE (Tris-Borate-EDTA) Buffer**

<b>Component</b>	<b>Amount</b>	<b>Concentration</b>
Tris Base	108 g	890 mM
Boric Acid	55 g	890 mM
EDTA	40 ml	20 mM

For 1X TBE this solution was diluted 1:10 and used for electrophoresis.

**Composition of 6X Loading Dye**

10 mM Tris-HCl (pH 7.6)  
0.03% bromophenol blue  
0.03% xylene cyanol FF  
60% glycerol  
60 mM EDTA

# APPENDIX E

## PLASMID MAPS

pDNR-Dual Donor Vector Information

PT3617-5

Sold as part of Catalog #K1677-1

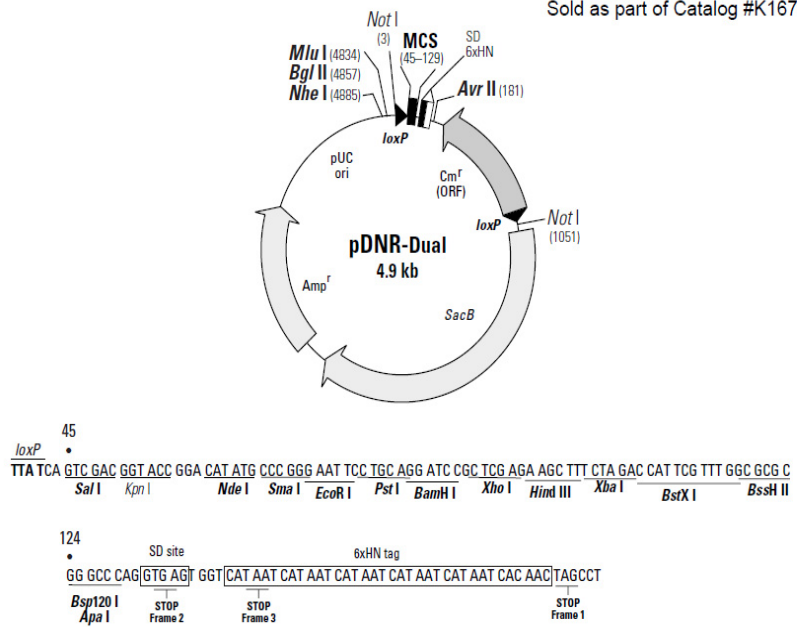


**Figure E.1** Map of pDNR Dual vector (image taken from CLONTECH® Laboratories Inc.)

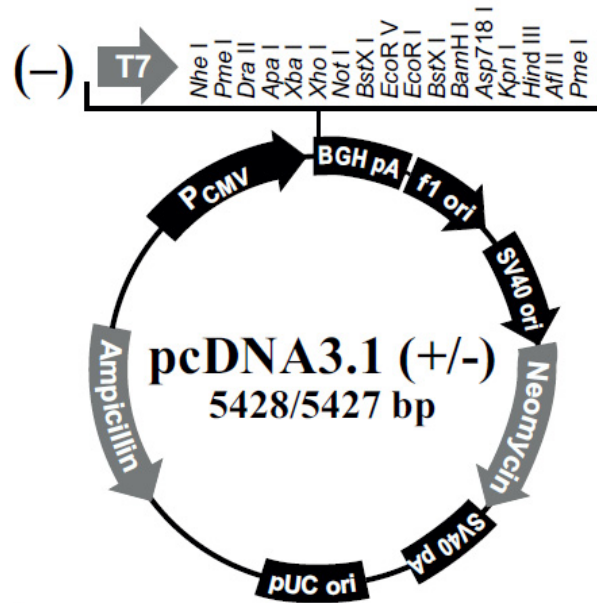


**Figure E.2** Map of pcDNA 3.1 (-) (image taken from Invitrogen® Life Technologies)

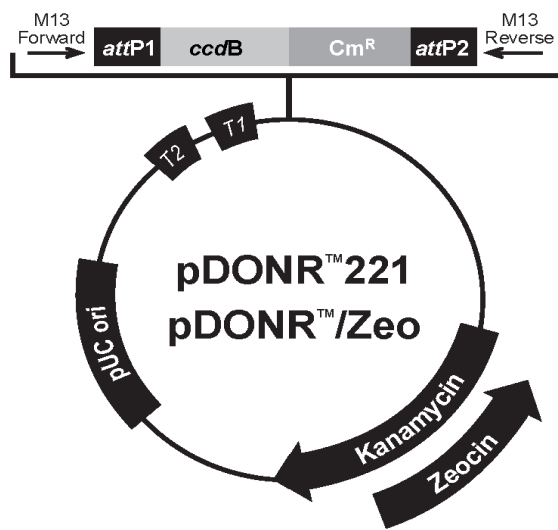


**Figure E.3** Map of pDONR 221 (image taken from Invitrogen® Life Technologies)

## APPENDIX F

### REPRESENTATIVE 3D OF RECEPTORS FUSED WITH FLUORESCENT PROTEINS

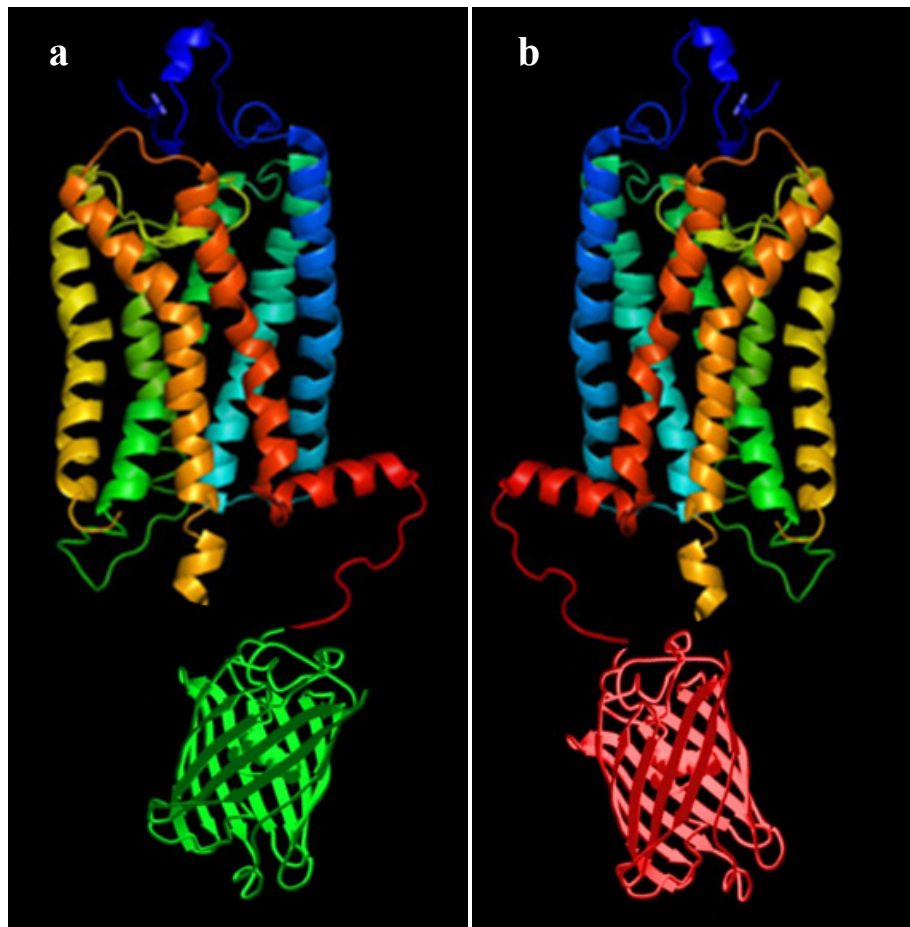


**Figure F.1** Representative 3D structures of receptor fusions **a)** with EGFP **b)** with mCherry constructed in this study

## APPENDIX G

### PRIMERS

#### Primers to amplify D2R cDNA with *SalI* and *HindIII* ends

Forward primer: 5'- ACGC<sup>G<sup>^</sup>TCGAC</sup> ATGGATCCACTGAATCTGTCCT - 3'

Reverse primer: 5'- ACGCA<sup>A<sup>^</sup>AGCTT</sup>ccGCAGTGGAGGATCTTCAGGAA - 3'

Shaded sequences show *SalI* and *HindIII* restriction cut sites; bases shown in small cases were added to preserve the frame. ACGC sequence was added at the 5' of both primers for restriction enzymes to be able to hold onto PCR product.

#### Primers to amplify mCherry cDNA with A<sub>2A</sub>R flanking ends

Forward primer for mCherry-A<sub>2A</sub>R:

5' - cccctggcccaggatggagcaggagtgtccATGGTGAGCAAGGGCGAGGAG - 3'

Reverse primer for mCherry-A<sub>2A</sub>R:

5' - cgcgccaacgaatggtctagaaagcttccTACTTGTACAGCTCGTCCATGCC - 3'

Small case bases at the 5' end of the forward primer belong to the last 30 bp of A<sub>2A</sub>R excluding stop codon. On the other hand, small case bases at the reverse primer correspond to the 30 bases on the pDNR-Dual vector which directly follow A<sub>2A</sub>R sequence. Capital letters show the primer sequences that anneal to mCherry gene.

### **Primers to amplify EGFP/mCherry with D2R flanking regions**

Forward primer for EGFP/mCherry-D2R:

5' – cgcaaggccttctgaagatcctccactgcATGGTGAGCAAGGGCGAGGAG – 3'

Reverse primer for EGFP/mCherry-D2R:

5' – ctgatcagcggtttaaacttaagcttccTACTTGTACAGCTCGTCCATGCC – 3'

Small case letters at the 5' end of the forward primer are the last 30 bp of D<sub>2</sub>R and those at the 5' are 30 bp of the pcDNA 3.1 (-) following D<sub>2</sub>R cDNA sequence. Capital letters are the parts that anneal to both EGFP and mCherry genes since these sequences are shared by both genes

### **Primers to amplify EGFP with A2AR flanking regions**

Forward primer for EGFP-A2AR

cccctggcccaggatggagcaggagtgtccttgATGGTGAGCAAGGGCGAGGAG

Reverse primer for mCherry-A2AR

ctgatcagcggtttaaacttaagcttccTACTTGTACAGCTCGTCCATGCC

Small case letters at the 5' end of the forward primer are the last 30 bp of A<sub>2A</sub>R and those at the 5' are 30 bp of the pcDNA 3.1 (-) following D<sub>2</sub>R cDNA sequence. Capital letters are the parts that anneal to EGFP coding sequence.